Two-Dimensional Finite Elasticity Analysis of the Stability of Multilayer Elastomeric Bearings

By

Juan C. Simo

and

James M. Kelly

University of California
Berkeley, California.

Report to:
Malaysian Rubber Producers Research Association

Report No. UCB/SESM-81/06
Structural Engineering and Sructural Mechanics
Department of Civil Engineering
University of California
Berkeley, California

November 1981

ACKNOWLEDGEMENTS

Support for this research was provided by the Malaysian Rubber Producers Research Association of Brichendonbury, England, as part of a program of research on the use of rubber bearings for the seismic protection of buildings. This support is gratefully acknowledged.

TABLE OF CONTENTS

1. INTRODUCTION

Rubber bearings are widely used in engineering applications. They are used as bridge bearings and as seating pads in concrete construction. High precision elastomeric bearings with very many layers are used in helicopters to replace fournal bearings where the motion is cyclic rather than rotational. A form of multilayer elastomeric bearing is used for dock fenders. They are widely used in Europe to isolate buildings from ground borne noise and there are recent applications of bearings to isolate buildings from the effects of earthquakes. The great advantage of elastomeric bearings is that they have no moving parts; they are not subject to corrosion and they are reliable, cheap to manufacture and need no maintanence.

Typical bridge bearings or acoustic isolation bearings for buildings consist of several layers of rubber bonded to steel plates which retain the rubber from bulging laterally under compressive load. In the case of seismic protection bearings there may be many thin layers of rubber bonded to steel plates. The constraint of the metal plates on the deformation of the rubber, with its almost incompressible character, is such that the resultant system has a very high compression stiffness while retaining the characteristic low shear stiffness of rubber. Such seismic isolation bearings function by decoupling the structure from the horizontal components of ground motion while simultaneously carrying the vertical load of the building.

It is a characteristic of the design of these bearings that the two phenomena of instability of the bearing and the reduction of the horizontal stiffness by vertical load, have an important effect on the design of the bearing. Although the bearings are typically quite short in comparison with their plan dimensions the very low shear stiffness introduces the possibility of buckling under compressive load and even if the axial buckling load is not approached, as should be the case in a well designed base isolation system, the shear stiffness of the element as a whole is reduced by the application of the compressive load.

The traditional approach to the stability analysis of rubber bearings has been to make use of Haringx's theory [1]. This theory is essentially a modification of the linearized theory of column buckling that takes into account the influence of shear deformation. This is accomplished by introducing Rankine's simplified kinematic assumption which, as it is well known, decouples the lateral deflection of a cross section from its angle of rotation by considering the latter as a new independent variable.

Within the scope of this one-dimensional approximation, the instability problem is thus treated as that of a homogeneous column with equivalent elastic properties given by the so-called apparent bending and shear stiffness. Various expressions for these variables, or related parameters (i.e.,apparent shear modulus, etc.) can be found in the literature ([2],[3] and references therein). Most of them involve the definition of a shape factor that takes into account the high confinement of the rubber, which is the key factor in the extremely high values found for the axial (compressive) stiffness. Probably, the most widely used expressions in design are those due to Gent and Lindley [4], and Gent and Mainecke [5]. Their analysis within the range of small deformations should be considered, as pointed out in [2], as an approximation.

The essential point in Haringx's treatment is that it predicts a reduction in the apparent lateral stiffness due to the presence of an axial load. However, for a given axial load the resultant shear stiffness is found to be a constant independent of the shear displacement as well as the amount of shear. Thus, for a given axial load the relationship between shear force and shear displacement is linear.

The theory due to Haringx and experimental measurements show fairly good agreement for moderate amounts of shear [6],[7]. However, further experimental work [7],[8] indicates that for a fixed axial load the shear load goes through a maximum as the shear deflection is further increased. The deflection at which this maximum occurs decreases with increasing constant axial load. The nature of this phenomenon, as pointed out in [7], is not clearly understood.

The purpose of this report is to provide an explanation of such phenomenon within the framework of finite elasticity. Furthermore a methodology is developed for the two dimensional analysis of elastomeric bearings subjected to very general loading an boundary conditions.

2. STABILITY OF ELASTOMERIC BEARINGS. EXPERIMENTAL RESULTS.

The stability phenomenon to be addressed in this report arose in the experimental testing of a set of seismic isolation bearings which were made for a shaking table test of a base isolation system. The bearings were used in this test with a 80,000 lb. structural model

The bearings were manufactured by the Andre Rubber Company Ltd. They were of natural rubber reinforced by steel plates and were made in modules incorporating two 1/4" thick layers of rubber and three 1/8" steel plates. A complete bearing incorporated 10 such modules. The modules are epoxied together but the epoxy is not used to transmit the shear forces between layers. Instead steel disks 1/4" are keyed into circular holes in the 1/8" steel plates on the top of one module and on the top of the one above. The bearings are keyed to the load cells at the bottom and to the steel frame at the top by the same disks. A typical bearing as installed is shown in Fig.1.

When the bearings were deflected horizontally to displacements of the order of four to five inches the horizontal force was observed to decrease with increasing displacement. Experimental force-displacement curves are plotted in Fig. 2 for different values of the axial load. The experimental procedure applies controlled displacements and measures the corresponding force. Under dead loading such a behavior would be considered as instability (Fig. 3).

It is important for the design of such seismic isolation bearings to ascertain the cause of this instability. A possible material instability that is a strain softening of the material was first explored by testing a single layer of the bearing. A description of the experimental test together with a discussion of this phenomenon can be found in Appendix I of this report. Another possible cause of instability was geometrical. It was observed that the end plates were subjected to unilateral restraints in the sense that during the testing of the bearings, the end conditions were such as to preclude the development of tension in the rubber. The end plates were located horizontally by the key disks but were not fixed against the loading platerns of the testing machine. Thus flexibility of the end plates of the bearings could allow a gap to form when the bearings were under vertical loads with large horizontal displacements.

In this report it will be shown that this roll-off at the end plates does produce an important reduction in the horizontal stiffness with increased load displacements and can lead to an eventual instability under constant axial load. The phenomenon will appear in any bearings which are under unilateral end constraints and may severe in the case of bearings with very flexible end plates. The two dimensional finite element formulation developed for the analysis of this problem in bearings could be used for designe purposes in allowing the end plates to be properly proportioned.

3. TWO DIMENSIONAL TREATMENT OF ELASTIC INSTABILITY PROBLEMS.

3.1. Basic considerations.

There are two reasons why the stability of a column subjected to axial and shearing loads should be considered in a two dimensional setting.. First, the effect of boundary conditions enforcing unilateral or partial end restraints, can only be properly considered in a two dimensional analysis. Secondly, in many practical instances, the length of the column is of the same order of magnitude as its transverse dimensions. In such cases, the assumption of a beam type of behavior might be questionable. In addition, by placing the two dimensional formulation in the framework of finite deformation elasticity, the consideration of instability phenomena follows inherently.

In the stability analysis of multilayer elastomeric bearings, good agreement has been found between experimental results and those predicted by the one dimensional theory of buckling due to Haringx, which accounts for shear deformation of the column. Therefore, a two dimensional analysis for this type of column must be consistent with Haringx's formulation whenever the assumptions of beam theory are expected to hold.

The results contained in Appendix II of this report, show that the equations of equilibrium in Haringx's treatment, in terms of the axial and shear forces and the bending moment, correspond to a consistent linearization of the equations of equilibrium of nonlinear elastostatics, whenever the kinematic assumptions of beam theory hold. Thus, with the appropriate two dimensional constitutive equations the theory of finite elasticity provides with an adequated framework for the two dimensional analysis of the stability of elastomeric bearings.

The development of a simple two dimensional constitutive model, consistent with the one dimensional theory, is the objective of this section. The linearized theory will be considered first, and the extension to the range of large displacements examined later.

3.2. Constitutive equations.

The main characteristic of a multilayer elastomeric bearing is that of a very low shear stiffness in comparison with the extremely high value taken by its compressive stiffness. Within the scope of the one dimensional theory, this type of behavior is modeled by considering a column with elastic properties given by its apparent compressive, bending and shearing stiffness.

3.2.1. Linear elasticity.

In the context of three dimensional elasticity, we shall follow a similar approach and, regarding the bearing as a composite material, model it as a transversally isotropic elastic material with its axis of symmetry being that perpendicular to the layers of the bearing.

The general constitutive equations for a transversally isotropic solid depend upon five independent constants [10]. We shall consider here a simplified version of this model given by

$$\begin{aligned} \sigma_{ij} &= \lambda \epsilon_{kk} \delta_{ij} + 2\mu \epsilon_{ij} \qquad (i=j) \\ \sigma_{ij} &= 2G \epsilon_{ij} \qquad\qquad\qquad (i \neq j) \end{aligned} \tag{3.1}$$

where λ, μ and G are independent elastic constants to be chosen so that this constitutive model adequately represents the behavior of the bearing.

The choice of the elastic constants.

Consider the bending problem of a transversally isotropic beam subjected to end loads contained in the plane perpendicular to the 3-axis. The exact solution of this problem [10] shows that

$$\sigma_{13} = \sigma_{23} = \sigma_{22} = \sigma_{33} = 0 \tag{3.2}$$

thus, equations (3.1) reduce to

$$\sigma_{11} = E\epsilon_{11} \qquad \sigma_{12} = G\epsilon_{12} \tag{3.3}$$

where the constants $E = \mu \dfrac{3\lambda+2\mu}{\lambda+\mu}$ and G are independent. The integration of equations (3.3) over the cross section of the beam yields the classical formulae of beam theory

$$M = EI\psi' \qquad V = GA_s\beta \tag{3.4}$$

where ψ and β are the bending and shear angles, and M and V the bending moment and shear force, respectively. Thus, denoting by K_b the apparent bending stiffness of the column [6], a suitable choice for E is provided by

$$E = \frac{K_b}{l} \tag{3.5}$$

In addition, the experimental results contained in Appendix I of this report, show that when a single unit of the bearing is subjected to a simple shear test, the relationship between shear deformation and shearing load is linear within a wide range of shear displacement †. Thus, the constant G in (3.1) can be chosen, either from an experimental test of this type, or from the data available in the literature [9].

Consistency of the constitutive model

The condition stating the positive definiteness of the strain energy function $W(\epsilon_{ij})$, is the basic restriction that continuum mechanics places on any constitutive model. More precisely, $W(\epsilon_{ij}) > 0$ for any symmetric second rank tensor ϵ_{ij}. This condition plays a key role in the analysis of the elastic stability.

Thus, it is important to assess whether the constitutive model given by equation (3.1) renders a positive definite strain energy W, particularly for values of $G < \mu$ which corresponds to the case of interest for elastomeric bearings.

Let us assume then that $\mu \geqslant G > 0$, and let $e_{ij} = \epsilon_{ij} - \frac{1}{3}\epsilon_{kk}$ be the deviatoric part of the strain tensor ϵ_{ij}. Since the strain energy function corresponding to the constitutive model (3.1) is given by

$$W = ½\lambda\{\epsilon_{kk}\}^2 + \mu\{\epsilon_{11}^2+\epsilon_{22}^2+\epsilon_{33}^2\} + 2G\{\epsilon_{12}^2+\epsilon_{13}^2+\epsilon_{23}^2\}$$

we have the inequality

$$W \geqslant ½(\lambda+\frac{2}{3}\mu)\{\epsilon_{kk}\}^2 + G\{e_{ij}e_{ij}\}$$

---

† This experimental results appears to confirm the suitability of the Mooney-Rivlin material for the modeling of the rubber layers.

Since ϵ_{kk} and e_{ij} can be specified independently, and

$$K = [\lambda + \frac{2}{3}\mu] > 0 \qquad G > 0$$

it follows that the strain energy W associated with the constitutive model (3.1) is in fact positive definite.

In conclusion, equation (3.1) provides a constitutive model which is both capable of representing the global behavior of a multilayered elastomeric bearing and physically consistent. The extension of this model to the range of large deformations will be examined next.

3.2.2. Extension to the range of large deformations.

The simplest extension of the constitutive model (3.1) to the range of large deformations, considers a constitutive relationship of the form

$$\begin{aligned} S_{IJ} &= \lambda^{*} E_{KK}\delta_{IJ} + 2\mu^{*} E_{IJ} \qquad (I=J) \\ S_{IJ} &= 2G^{*} E_{IJ} \qquad (I \# J) \end{aligned} \tag{3.6}$$

where S_{IJ} and E_{IJ} are the components of the second Piola-Kirchhoff stress tensor **S** and the Lagrange tensor **E**, respectively [11],[12].

The important point to be noticed however, is that the elastic constants λ^{*}, μ^{*} and G^{*} do not necessarily coincide with the constants λ, μ and G in equation (3.1) corresponding to the linear theory.

Physically meaningful expressions for these elastic constants can be obtained by considering again the simple problem of the bending of a beam by applied end forces.

The choice of the elastic coefficients

A typical element of the beam subjected to end forces and no distributed loads, undergoing large displacements, is represented in Fig.4. We have neglected the warping of the cross section, and assumed that plane section normal to center line remain plane after the deformation has taken place.

Let σ and τ be the normal and tangential stresses acting on the deformed cross section.

The stresses S_{11} and S_{12} are related to σ and τ by

$$S_{11} = \sigma \qquad S_{12} = -\sigma\beta + \tau \tag{3.7}$$

where $\beta = v' - \psi$ is the shear angle, plotted in Fig.4. The equivalent expressions in terms of the axial force N and the shear force V are

$$\int_A S_{11} dA = N \qquad \int_A S_{12} dA = -\beta N + V \tag{3.8}$$

and the components E_{11} and E_{12} of the Lagrange strain tensor **E** can be approximated by

$$E_{11} = u' - y\psi + \frac{1}{2} v'^2 \qquad E_{12} = \frac{1}{2}\beta \tag{3.9}$$

The proof of equations (3.7) to (3.9) can be found in Appendix II of this report.

It has already been pointed out that the linear relationship between shear displacement and applied shear force holds within a large range of shear displacements. Thus, it is reasonable to assume that the relation

$$V = GA_s\beta \tag{3.10}$$

still holds in the range of large deformations.

By equilibrium considerations, the axial force N acting on the cross section of the deformed beam is given by

$$N = -P - Q\psi \tag{3.11}$$

where P is the compressive load and Q the transversely applied load at the end of the beam. Neglecting higher order terms, $\beta N = -\beta P$, and (3.8) reduces to

$$\int_A S_{12} dA = \left(\frac{P}{A_s} + G \right) A_s \beta \tag{3.12}$$

which is the counterpart, in the range of large displacements, of the equation

$$\int_A \sigma_{12} dA = GA_s\beta$$

valid for small deformations. Noting that $E_{12} = ½\beta$, equation (3.12) shows that the coefficient G^* in the extended constitutive model (3.6) is, within this first order approximation, given by

$$G^* = G + \frac{P}{A_s} \tag{3.13}$$

Finally, since

$$M = -\int_A y\sigma\, dA = -\int_A S_{11} y\, dA \tag{3.14}$$

the first of equation (3.5) together with (3.9) gives again

$$M = E^{*} I \psi' \tag{3.15}$$

which shows that the elastic constant E^{*} can be taken equal to E; i.e:

$$E^{*} = E = K_b / I \tag{3.16}$$

It should be noticed that by equation (3.7), the value of the stress component S_{12} can never coincide with the tangential stress τ acting on the deformed cross section unless the axial load $P = 0$, as opposed to the case of small displacements in which $\sigma_{12} = \tau$. Actually, it can be shown that S_{12} gives the tangential stress acting on a plane normal to the deformed center line which is, therefore, rotated an angle β with respect to the deformed cross section. Since $2E_{12}$ gives the actual shearing β of the section, it follows that G^{*} can never coincide with G unless $P = 0$. The expression for G^{*} given by equation (3.13), is consistent with this observation.

3.3. The two-dimensional formulation.

The two dimensional formulation proposed in this section, amounts to solving the equations of equilibrium of nonlinear elasticity given by (see Appendix II)

$$Div(\mathbf{FS}) + \rho_o \bar{\mathbf{b}} = 0 \tag{3.17}$$

where $\mathbf{F}$ is the deformation gradient, and $\bar{\mathbf{b}}$ the body forces, together with the constitutive equations given by (3.6) and the appropriate boundary conditions. Equations (3.13) and (3.16) provide expressions for the elastic coefficients involved in (3.6) suitable for a global modeling of the behavior of an elastomeric bearing. Clearly, the resulting boundary value problem is highly non linear and must be solved numerically.

All that is needed to complete the formulation is a stability condition which can easily be implemented in the solution procedure.

4. SOLUTION PROCEDURE. STABILITY CONDITION.

In this section we present the solution procedure for our two dimensional formulation of elastic stability problems. The procedure uses instead of equation (3.17) its variational formulation in terms of the principle of virtual work. This form of the equations of equilibrium is the most convenient both for computational purposes and for the incorporation of the classical stability condition.

We examine first the case of dead loading. The extension to the case in which part of the boundary is subjected to unilateral constraints is considered next.

4.1. Solution procedure and stability condition for dead loading.

Let B be the undeformed configuration of the body of interest, $\mathbf{x} = \Phi(\mathbf{X})$ the final position of a particle initially located at $\mathbf{X}$ in B, and $\mathbf{u} = \mathbf{x}-\mathbf{X}$ the displacement vector. The deformation gradient and Lagrangian strain tensor [11] defined in Appendix II, take then the form

$$\mathbf{F} = \mathbf{I} + \nabla\mathbf{u} \qquad \mathbf{E} = \frac{1}{2}[\nabla\mathbf{u} + \nabla\mathbf{u}' + \nabla\mathbf{u}'.\nabla\mathbf{u}] \tag{4.1}$$

In addition, let ∂B_t the part of ∂B, the boundary of B, where the tractions $\bar{\mathbf{t}}$ are prescribed, and ∂B_d that part of ∂B where the displacements are prescribed. Denoting by $\delta\mathbf{u}$ an arbitrary admissible variation, the principle of virtual work takes the form

$$G(\mathbf{u},\delta\mathbf{u}) = \int_B (\mathbf{FS}.\nabla\mathbf{u})\nabla(\delta\mathbf{u})\,dV - \int_B \rho_o\bar{\mathbf{b}}.\delta\mathbf{u}\,dV - \int_{\partial B_t} \bar{\mathbf{t}}.\delta\mathbf{u}\,dS = 0 \tag{4.2}$$

The non-linearity of this equation is not explicit but rather rests on the choice of the constitutive equation

$$\mathbf{S} = \hat{\mathbf{S}}(\mathbf{E}) \tag{4.3}$$

For the simple constitutive model proposed in section 3. (eq.(3.6)) the stresses $\mathbf{S}$ are a linear function of the strains $\mathbf{E}$. Nevertheless due to equation (4.1), the dependence of $\mathbf{S}$ on the displacements $\mathbf{u}$ is non linear.

Introducing the total potential energy functional Π, the solution of the boundary value problem posed by equations (4.2) and (4.3) can be characterized by the single equation [12]

$$\delta\Pi(\mathbf{u}) = \frac{d}{d\alpha}\{\, \Pi(\mathbf{u} + \alpha\delta\mathbf{u})\,\}|_{\alpha=0} = 0 \tag{4.4}$$

which is simply a restatement of the virtual work equation (4.2) with $\mathbf{S}$ given by (4.3).

Stability condition

The classical stability condition, the energy criterium [11],[12], states that a solution $\mathbf{x} = \Phi(\mathbf{X})$ of equation (4.4) is stable whenever Π achieves a minimum at Φ. Thus, stable solutions are characterized by

$$\delta^2\Pi(\mathbf{x}) > 0 \tag{4.5}$$

In terms of the elastic moduli $\mathbf{C}$ (the second elasticity tensor) defined by

$$\mathbf{C} = \frac{\partial \mathbf{S}}{\partial E} = \frac{\partial^2 W(\mathbf{E})}{\partial \mathbf{E}\partial \mathbf{E}} \tag{4.6}$$

where W is the strain energy function, the condition given by equation (4.5) takes the form

$$\begin{aligned} &\int_B \{F_{iA}\, C_{AIBJ}\, F_{jB} + S_{IJ}\,\delta_{ij}\}\,\delta u_{i,I}\,\delta u_{j,J}\, dV = \\ &\int_B \{C_{ABCD}\,\delta E_{AB}\,\delta E_{CD} + S_{IJ}\,\delta^2 E_{IJ}\}\, dV > 0 \end{aligned} \tag{4.7}$$

in which majuscule and minuscule subindices refer to initial and current configurations, respectively. Yet, a more compact expression of condition (4.5) is possible by introducing the (first) elasticity tensor, defined by

$$\mathbf{A} = \frac{\partial^2 W(\mathbf{F})}{\partial \mathbf{F}\partial \mathbf{F}} = \frac{\partial \mathbf{P}}{\partial \mathbf{F}} \tag{4.8}$$

from equation (4.4) condition (4.5) reduces to

$$\int_B (\mathbf{A}\,\delta\mathbf{u}).\delta\mathbf{v}\; dV = \int_B A_{iIjJ}\,\delta u_{i,I}\,\delta v_{j,J}\, dA > 0 \tag{4.9}$$

for arbitrary variations $\delta\mathbf{u},\delta\mathbf{v}$.

It should be noticed that if the tensor $\mathbf{C}$ is positive definite, as in the model defined by equation (3.6), the term containing $\mathbf{C}$ in (3.7) is greater than zero since $\delta\mathbf{E}$ is symmetric. Thus, an eventual violation of the stability condition can only be due to the term containing the stresses $\mathbf{S}$, the so-called geometric term.

We show below that the stability condition (4.9) plays an key role in the solution of the nonlinear problem (4.4) by an iterative linearization procedure.

Solution procedure

In a typical numerical solution, the principle of virtual work is discretized using finite element techniques. The resulting nonlinear system is then solved by Newton's method, an iterative linearization process. This approach is equivalent to considering the global non linear problem as a sequence of linear problems, regardless of the specific technique employed in the numerical solution. At each intermediate configuration, say $\mathbf{x}^{(n)} = \Phi^{(n)}(\mathbf{X})$, we obtain an incremental linear displacement $\mathbf{u}^{(n)}$ satisfying for arbitrary variations $\delta\mathbf{u}^{(n)}$ about $\mathbf{x}^{(n)}$, the linear problem

$$\int_B (\mathbf{A}^{(n)}.\nabla\mathbf{u}^{(n)}).\nabla\delta\mathbf{u}^{(n)}dV = \int_B \rho_o\bar{\mathbf{b}}.\delta\mathbf{u}^{(n)}dV + \int_{\delta B_t} \bar{\mathbf{t}}.\delta\mathbf{u}^{(n)}dS - \int_B (\mathbf{FS})^{(n)}.\nabla\delta\mathbf{u}^{(n)}dV \tag{4.10}$$

obtained from (4.2) and (4.3) by standard linearization techniques [13]. It is well known [12] from the theory of elasticity, that the solution of (4.10) is possible only when the left hand side of (4.10) does not vanish. From equation (4.9) this condition amounts to the requirement of a stable intermediate configuration $\mathbf{x}^{(n)}$.

Thus, if the final configuration is stable an algorithm of the form $\mathbf{x}^{(n+1)} = \mathbf{x}^{(n)} + \mathbf{u}^{(n)}$ will converge to the solution $\mathbf{x} = \Phi(\mathbf{X})$ provided that at each step the right hand side of (4.10), the out-of-balance forces, is small. This condition can always be achieved in practice by applying the external loads in sufficiently small increments.

4.2.1. Numerical solution.

A numerical solution procedure of the nonlinear problem (4.4) based on an iterative solution of the linear problem (4.10) can be easily implemented using the finite element method. In reference [17] it is shown that the discrete analog of equation (4.10) takes the form

$$\mathbf{K}_t^{(n)}\mathbf{U}^{(n)} = \mathbf{R}^{(n)} \tag{4.11}$$

where $\mathbf{K}^{t^{(n)}}$ is the tangent stiffness matrix, $\mathbf{U}^{(n)}$ the vector of nodal displacements and $\mathbf{R}^{(n)}$ the residual force vector. The superscript (n) refers to an intermediate configuration. We have given explicit expressions for these arrays in [17]. The dimension of the linear system of equations (4.11) is the number of degrees of freedom used in the discretization process times the spatial dimension of the problem.

The stability condition (4.9) reduces for this discrete problem to the positive definiteness of the tangent stiffness matrix $\mathbf{K}_t^{(n)}$. If this condition does not hold for arbitrarily small increments of the external loads we regard the configuration as unstable.

Finally, according to equation (4.7) the tangent stiffness can be written in the form

$$\mathbf{K}_t = \mathbf{K}_{tO} + \mathbf{K}_{tG} \tag{4.12}$$

where $\mathbf{K}_{tO}$, the initial stiffness, is computed from the term containing $\mathbf{C}$ in (4.7) and $\mathbf{K}_{tG}$, the geometric stiffness, from the term containing $\mathbf{S}$. The explicit expression in matrix notation of the elastic moduli $\mathbf{C}$ for the constitutive model (3.4) is

$$[C_{ABCD}] = \begin{bmatrix} \begin{bmatrix} \lambda^* + 2\mu^* & 0 \\ 0 & \lambda^* \end{bmatrix} & \begin{bmatrix} 0 & G^* \\ G^* & 0 \end{bmatrix} \\ \begin{bmatrix} 0 & G^* \\ G^* & 0 \end{bmatrix} & \begin{bmatrix} \lambda^* & 0 \\ 0 & \lambda^* + 2\mu^* \end{bmatrix} \end{bmatrix}. \tag{4.13}$$

where the last two indices position the submatrix and the first two, one of its elements.

As noted before, the matrix $\mathbf{C}$ given by (4.13) is positive definite. Therefore, the initial stiffness matrix $\mathbf{K}_{tO}$ is always positive definite and any eventual instability must come from the geometric stiffness $\mathbf{K}_{tG}$.

It should also be noted that even for a general constitutive model all sources of instability can be encompassed by this simple formulation.

The numerical solution procedure discussed above, has been implemented in the general purpose finite element computer program FEAP, listed in Chap. 24 of reference [16]. The practical implementation does not differ substantially from that described in [17], except for the different form of the constitutive model. In the present context it is more convenient to compute the elasticity tensor **A** from the relation

$$A_{iIjJ} = C_{AIBJ} F_{iA} F_{jB} + S_{IJ} \delta_{ij}$$

where C_{IAJB} is given by (4.14) and S_{IJ} by (3.6). The explicit expression for the tangent stiffness matrix follows then at once using standard finite element techniques [16], [17].

4.2. Extension to the case of unilateral constraints.

We consider in this section the extension of our previous development to the case in which unilateral constraints are present. The bearing represented in Fig.5 is taken as the model problem.

Let ∂B_c be the part of the boundary ∂B subjected to the unilateral restraint condition. Notice that ∂B_c is always known in advance, as opposed to the case of a general contact problem in which ∂B_c is in general unknown. Fig.6 shows ∂B_c for our model problem.

It will also be assumed that the displacements on ∂B_c are small so that the units vector normal to this part of the boundary before and after the deformation are approximately equal. This assumption is reasonable for the deformations observed in multilayer elastomeric bearings. Thus, the displacements **u** on the boundary ∂B_c satisfy the kinematic conditions

$$u_2 \geqslant 0 \qquad \textit{if } u_2 = 0 \textit{ then } u_1 = 0 \quad \textit{on } \partial B_c \tag{4.14}$$

that characterize the geometry of the unilateral constraint. (Fig.6).

In a variational formulation these are the only conditions that need be considered. They place on the admissible variations the restrictions

$$\delta u_2 \geqslant 0 \qquad \textit{if } \delta u_2 = 0 \textit{ then } \delta u_1 = 0 \quad \textit{on } \partial B_c \tag{4.15}$$

The solution for this type of problems is then characterized as the deformation that renders a minimum of the total potential energy for all admissible variations $\delta\mathbf{u}$ satisfying (4.15). Due to conditions (4.15) the principle of virtual work (or alternatively, equation (4.4)) takes the form of an inequality rather than an equality; i.e

$$\delta\Pi(\mathbf{u}) = \frac{d}{d\alpha}[\Pi\{\mathbf{u}+\alpha(\delta\mathbf{u}-\mathbf{u})\}]|_{\alpha=0} \geqslant 0 \tag{4.16}$$

We note that even within the limits of the linear theory of elasticity, the problem posed by equation (4.16) is nonlinear.

If equation (4.16) is consistently linearized a result analogous to that of equation (4.10) is obtained with the equality sign replaced by an inequality. It can be shown [14] that a solution for this problem is possible only when condition (4.9) holds.

For computational purposes, however, inequality (4.16) is not the most convenient formulation of the problem with unilateral constraints. It is preferrable instead to include the unknown contact pressures acting on ∂B_c explicitly in the formulation by means of Lagrange multipiers. Thus, we consider a modified total potential energy functional of the form

$$\Pi^* = \Pi - \int_{\partial B_c} \lambda . \mathbf{u} dS \tag{4.17}$$

where Π is the regular total potential energy, and the Lagrange multipiers λ the unknown contact pressures. The inequality constraints (4.15) no longer need be enforced on the admissible variations $\delta\mathbf{u}$. They simply satisfy the usual condition of vanishing on ∂B_d.

The virtual work expression associated with (4.17) can then be discretized using standard finite element techniques. The procedure for the terms deriving from Π has already been discussed in the previous section. A detailed discussion of the finite element discretization for the terms involving the Lagrange multipiers λ can be found in [17] and references therein.

Numerical examples illustrating the formulation presented in this section will be considered next.

5. NUMERICAL EXAMPLES.

Two numerical examples are included in this section. The first one illustrates the ability of the formulation presented in the previous section to reproduce the results of Haringx's theory when the elastic constant G^* in constitutive model given by (3.6) is chosen according to (3.13), and the assumptions of beam theory hold. The theoretical justification of this fact can be found in Appendix II. The second example shows the importance of unilateral constraints in the elastic stability of a short column.

Both examples correspond to a generalized state of plane stress. Therefore, since $S_{33} = 0$, the constant λ^* in the constitutive model (3.6) is replaced as in the linear theory by

$$\lambda^* \rightarrow \lambda^*_{eq} = \frac{2\lambda^*\mu^*}{\lambda^* + 2\mu^*} \tag{5.1}$$

Except for this substitution, the constitutive model (3.6) remains unaltered. In terms of the generalized Poisson modulus, defined by $\nu^* = -\dfrac{E_{22}}{E_{11}}$ in a homogeneous extension along axis-1, the elastic constants in (3.6) take the simple form (the subscript "eq" is dropped)

$$\lambda^* = \frac{\nu^*}{1-\nu^{*2}}E \qquad \mu^* = \frac{1}{2(1+\nu^*)}E \qquad G^* = G + \frac{P}{A} \tag{5.2}$$

where E is the apparent Young modulus given by (3.16) and G the shear modulus. P and A are the applied axial force and effective area, respectively.

The solutions for the numerical examples presented were obtained by a Newton-Ralphson iteration within each incremental loading step, in accordance with the formulation discussed in section 4. The capabilities of the general purpose computer program FEAP easily allow for this type of algorithm.

Example 1.

A slender beam with ratio $\dfrac{length}{width} = 10$ and left end clamped, is subjected to an axial and transversal load applied both on its right end. The constants E and G are taken to be: E = 10^6 and G = 500. The finite element discretization consists of five 9-node isoparametric elements of equal length, as shown in Fig. 7. The values of the constants λ^*, μ^* and G^* computed from

E and G through (5.2), are also included in Fig. 7. For this problem, the value of the buckling load predicted by Haringx's theory is $P_{crit} = 794.31$

A typical relationship between lateral load and tip deflection was found to be linear for a given value of the axial load, in agreement with Haringx's theory. The values found for the lateral stiffness as a function of the applied axial load are shown in Fig. 8. These computed results are in close agreement with those predicted by Haringx's theory, for values of the axial load P as close to the buckling load as P = 720.

Example 2.

As a second example, a beam with ratio $\frac{length}{width} = 1.8$ and left end clamped is presented to illustrate the effect of unilateral constraints. The right end of the beam is subjected to resultant axial and lateral loads, and is constrained by the condition that no tractions can occur at this end. This unilateral constraint, discussed in the previous section, is modeled by means of the contact element described in reference [15]. The finite element mesh and the location of the contact elements are shown in Fig. 9, together with the values of the different elastic constants.

The computed lateral load-tip deflection curves for different values of the axial load are depicted in Fig. 10. These curves are straight lines, with slopes in close agreement with the values predicted by Haringx's theory, up to the value of the lateral load for which roll-off of the right end starts to occur. A progressive reduction of the lateral tangent stiffness is then observed with further increments of the lateral load. The last computed point in the curves of Fig. 10 corresponds to the value of the lateral load for which the tangent stiffness matrix becames singular. According to the formulation presented in the previous section, the configuration of the beam for this value of the axial load should be regarded as unstable. The lateral tangent stiffness is approximately zero for this value of the axial load.

It should be noted that the reduction in lateral stiffness due to the presence of the unilateral constraint becomes more severe with increasing axial load, as illustrated in Fig.10.

6. CONCLUSIONS

A formulation for the solution of elastic stability problems embedded in the general setting of two-dimensional finite elasticity has been presented, together with two dimensional constitutive equations capable of modeling the typical behavior of multilayer elastomeric bearings. This constitutive model is an extension to the range of large displacements of the constitutive equations for a transversally isotropic solid. Physically meaningful expressions for the elastic constants involved in the model have been derived. It has been shown that the resulting formulation is in agreement with that due to Haringx when the assumptions of beam theory hold. The numerical examples presented illustrate this conclusion.

In addition, boundary conditions enforcing unilateral end constraint have been discussed. They play a key role in the elastic stability of the bearing, as illustrated in the numerical example presented. This type of boundary condition, rather than a form of material instability, explains the progressive reduction in lateral stiffness and eventual instability observed in the experimental testing of seismic isolation bearings.

REFERENCES

[1] Haringx, J. A., "On Highly Compressive Helical Springs and Rubber Rods and Their Applications to Free Mountings," Parts I, II ,III. *Philips Res. Reports. 1948-1949.*

[2] Beatty, M. F., "Elastic Stability of Rubber in Compression," In *Finite Elasticity*, Ed. R. S. Rivlin, *ASME, AMD, Vol. 27, pp. 125-150, (1977)* Winter Annual Meeting ASME, Atlanta, Ga., Nov. 27-Dec. 2, 1977.

[3] Roeder, C. W. and J. F. Stanton, "Elastomeric Bearings - Design Construction and Materials," *Interim Report, Oc. 1981* Department of Civil Engineering, University of Washington. Seattle, Washington.

[4] Gent, A. N. and P. B. Lindley, "The Compression of Bonded Rubber Blocks," *Proc. Instn. Mech. Engrs. Vol. 173, No. 3, pp.111-122. (1959)*

[5] Gent, A. N and E. A. Meinecke, "Compression, Bending and Shear of Bonded Rubber Blocks," *Polymer Engineering and Science, Vol.10, No.1, pp.48-53. (1970)*

[6] Gent, A. N., "Elastic Stability of Rubber Compression Springs," *J. Mech. Engng. Sc. Vol. 6, No. 4, pp. 318-326. (1964).*

[7] Derham, C. J. and A. G. Thomas, "The Design of Seismic Isolation Bearings," In *Control of Seismic Response of Piping Systems and Other Structures by Base Isolation.* Ed. J. M . Kelly. *Report No. UCB/EERC-81/01. January, 1981*

[8] Kelly, J. M., K. E. Beucke and M. S. Skinner, "Experimental Testing of a Friction Damped Aseismic Base Isolation System with Fail-Safe Characteristics," *Report No. UCB/EERC-80/18, July 1980.*

[9] Lindley, P. B, "Engineering Design with Natural Rubber," *Natural Rubber Technology Bulleting*, Malaysian Rubber Producers Research Association, (1974)

[10] Lekhnitskii, S. G., **Theory of Elasticity of an Anisotropic Elastic Body.** Holden-Day, Inc. S. Francisco, 1963

[11] Truesdell, C. and W. Noll, **The Non-Linear Field Theories.** Handbuch der Physik, Vol. III/33. Ed. S. Flugge. Springer-Verlag 1965.

[12] Gurtin, M. **Topics in Finite Elasticity.** Society for Industrial and Applied Mathematics. Philadelphia, Pen. (1981)

[13] Hughes, T. J. R. and K. S. Pister, "Consistent Linearization in Mechanics of Solids and Structures" *Computer & Structures, Vol. 8, pp. 391-397. (1978)*

[14] Duvaut, G. and J. L. Lions. **Les Inequations en Mecanique et en Physique.** Dunod, Paris 1972.

[15] Hughes, T. J. R., R. L. Taylor and J. L. Sackman, "Finite Element Formulation and Solution of Contact Impact Problems in Continuum Mechanics," Parts I, II ,III. *SESM reports No . 74-3 (1974), No. 75-3 (1975), No. 75-7 (1975).* University of California, Berkeley.

[16] Zienkiewicz, O. **The Finite Element Method.** Third Edition, MacGraw-Hill (1977)

[17] Simo, J. C. and R. L. Taylor, "Penalty Formulations for Rubber-Like Elasticity," *Report No. UCB/SESM-81/03, Nov. 1981. University of California, Berkeley. (1981)*

[18] Jaunzemis, W. **Continuum Mechanics.** MacMillan Co., New York 1962.

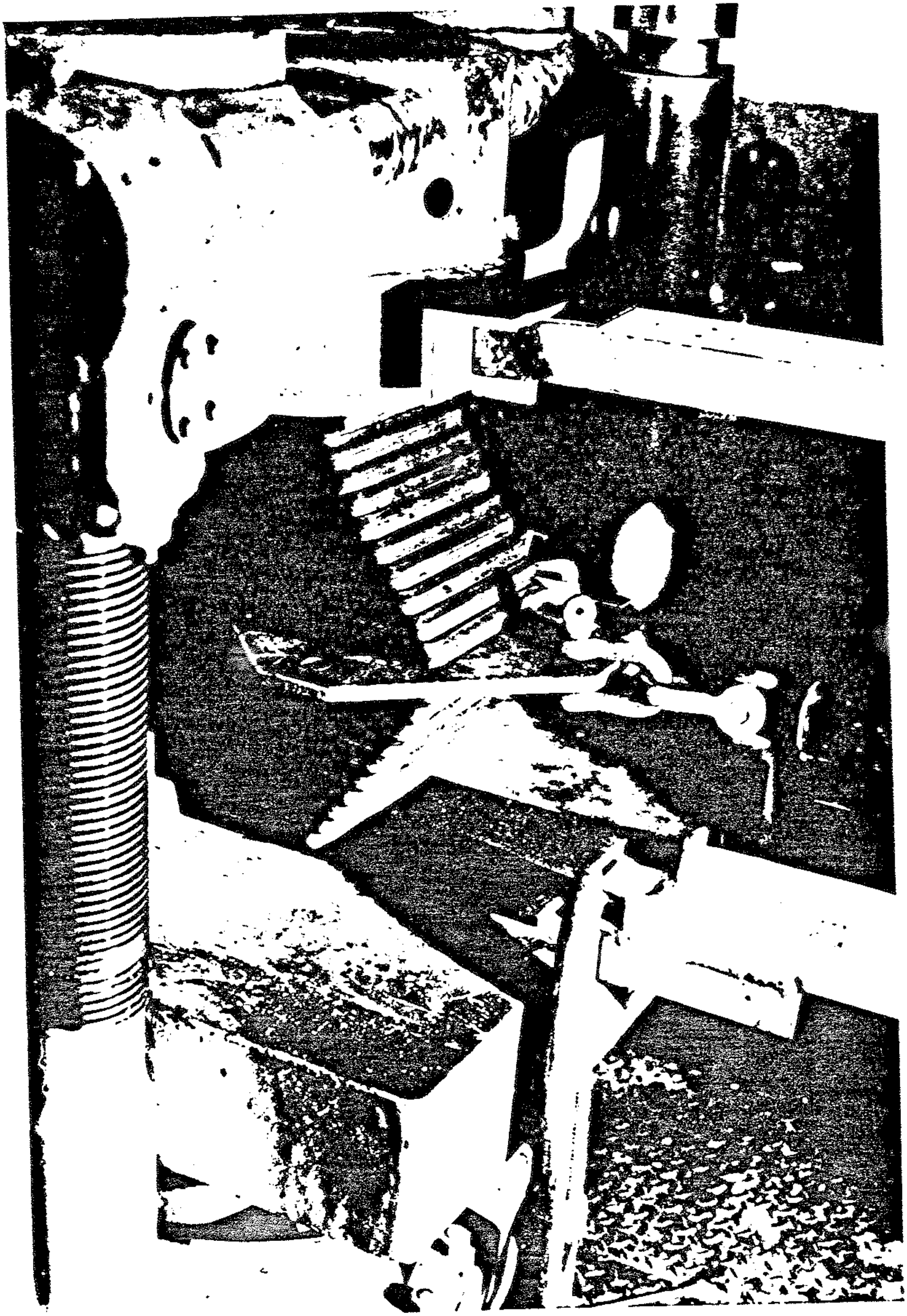

Fig.1 . Experimental test of an elastomeric bearing.

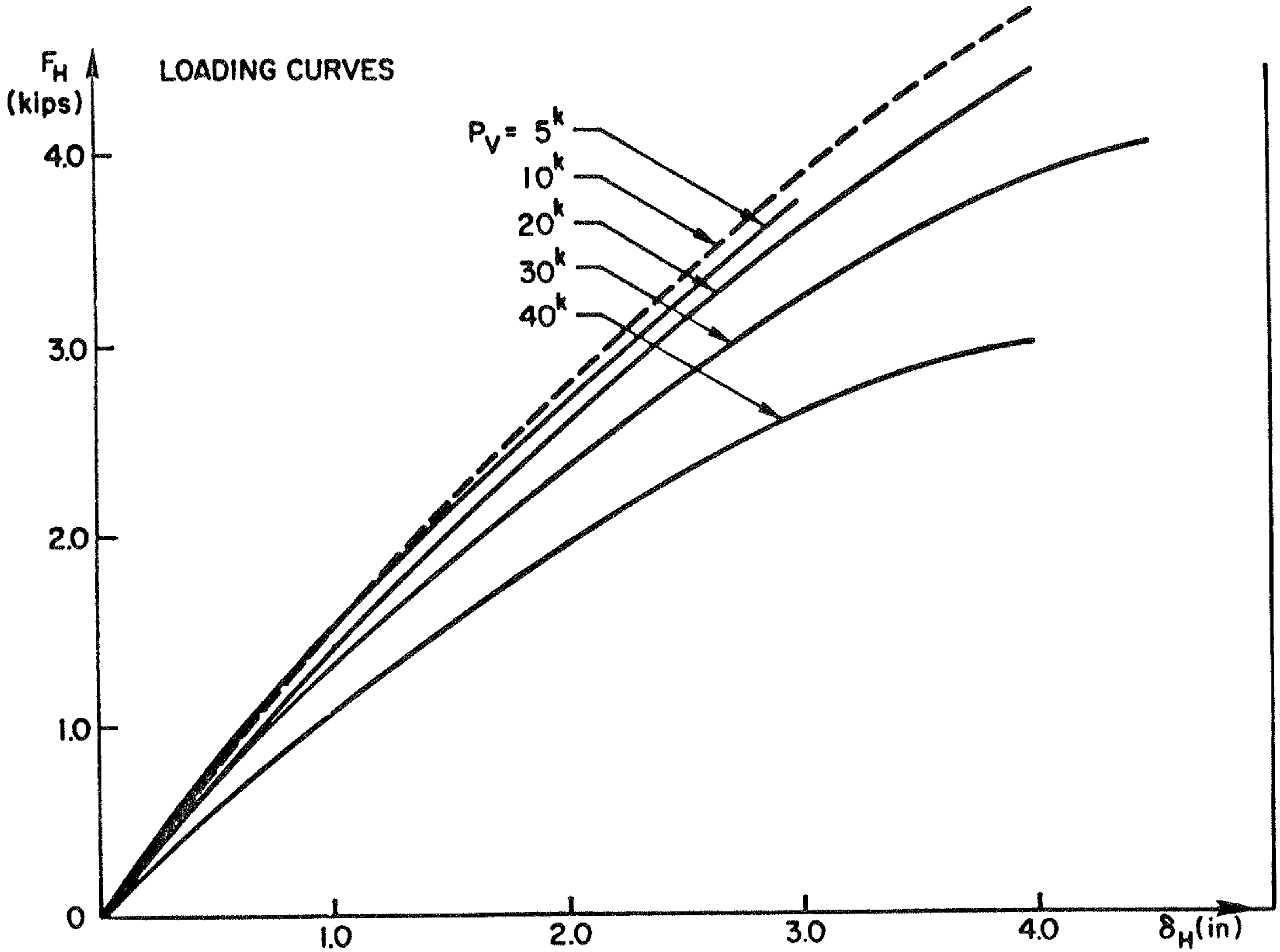

Fig. 2. Experimental Load-Displacement curves for a multilayer elastomeric bearing.

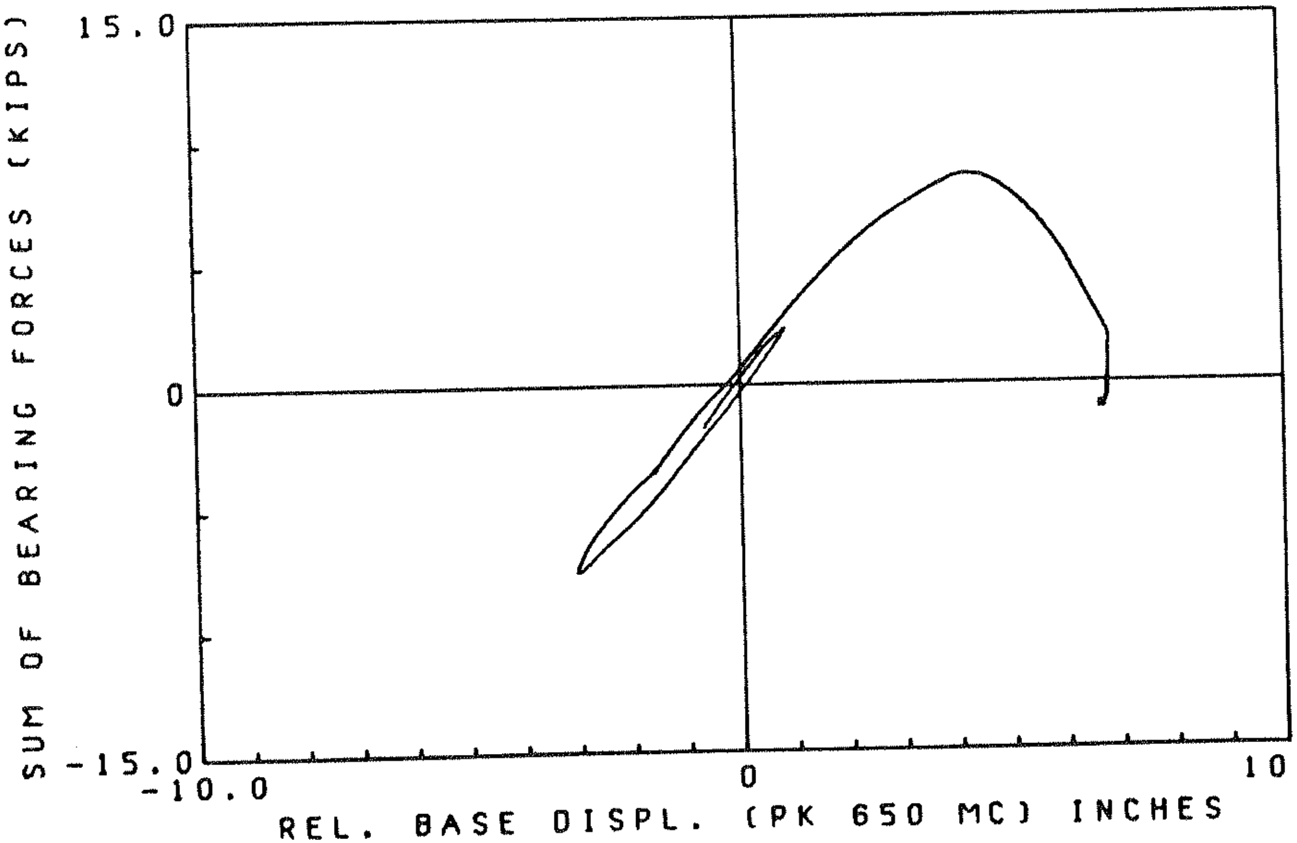

Fig.3. Observed instability in elastomeric bearings.

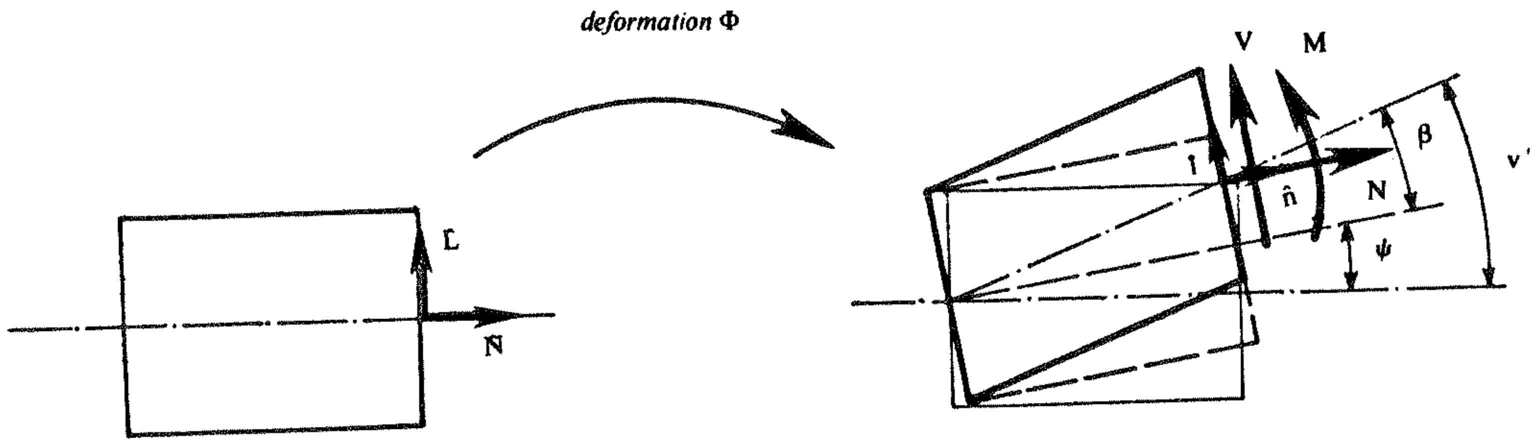

undeformed configuration

deformed configurtion

Fig.4. Geometry of a typical element of a beam.

ψ = Bending angle.

β = Shear angle.

v' = Slope of the deformed center line.

M,N,V = Resultant forces.

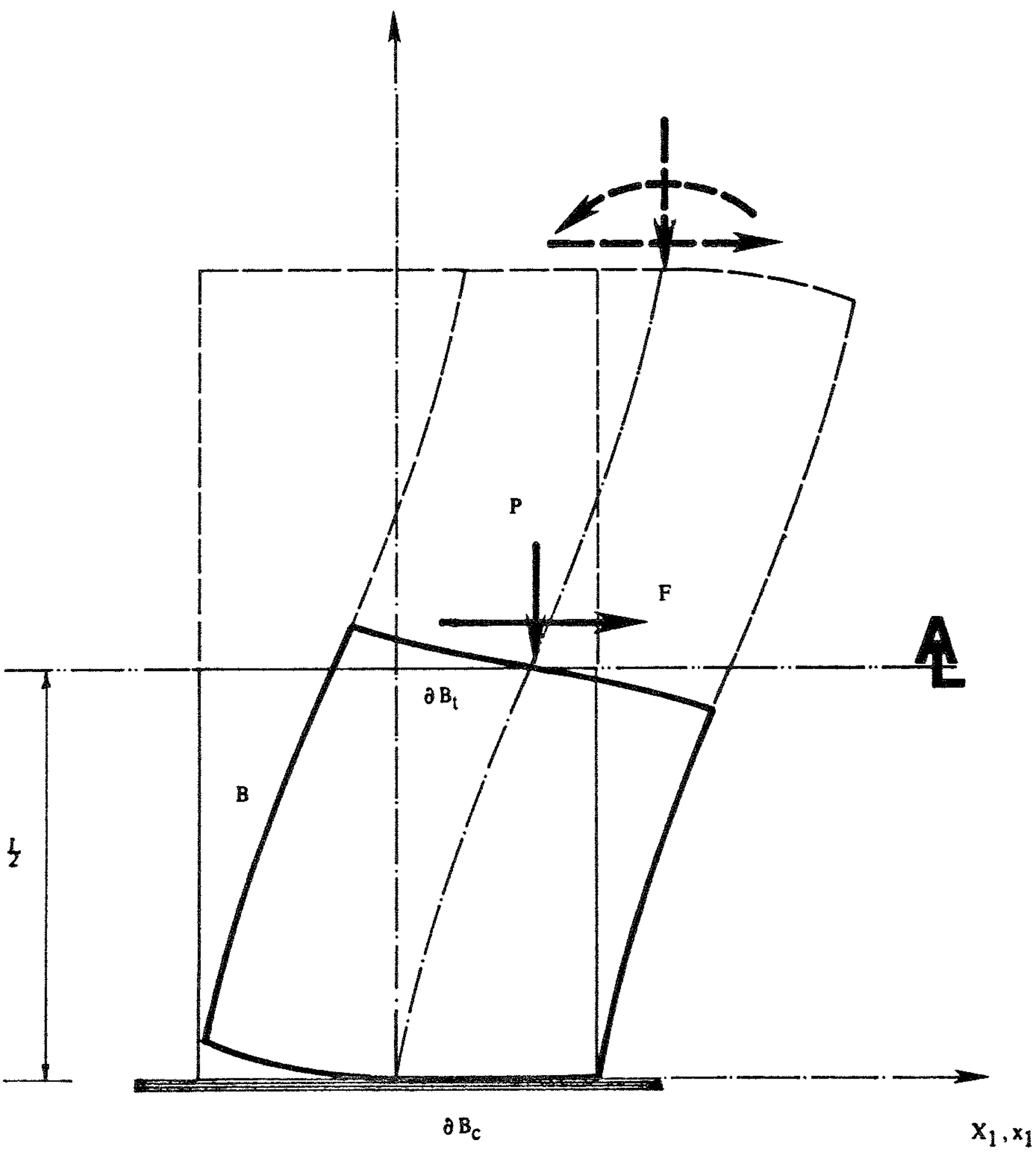

Fig.5. Deformation pattern of a typical elastomeric bearing.

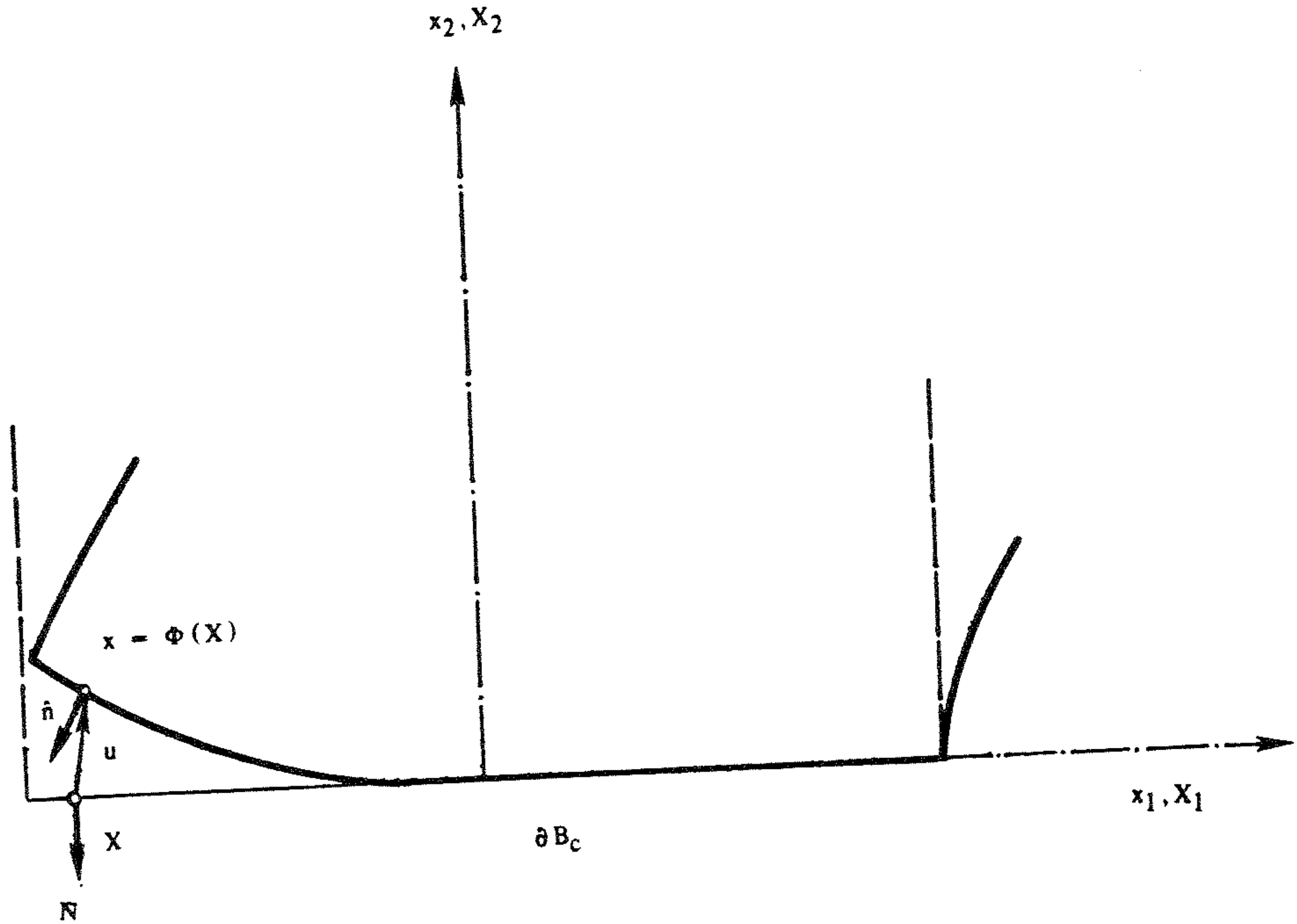

$$\left.\begin{array}{l} u_2 \geq 0 \\ \text{if } u_2 = 0 \text{ then } u_1 = 0 \end{array}\right\} \quad \text{on } \partial B_c$$

Fig.6. Geometry associated with the unilateral constraint.

Beam properties

$E = 1000000$

$G = 500$

Material properties

$\lambda^* = 266666.67$

$\mu^* = 400000$

$\nu^* = .25$

$G^* = 500. + \frac{P}{A}$

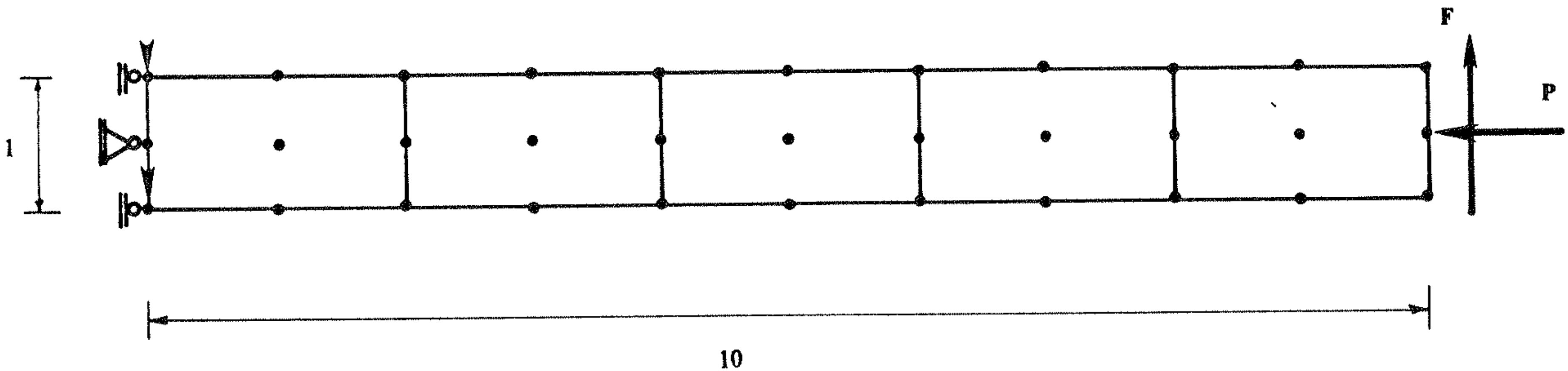

Fig. 7. Material properties and mesh for example 1.

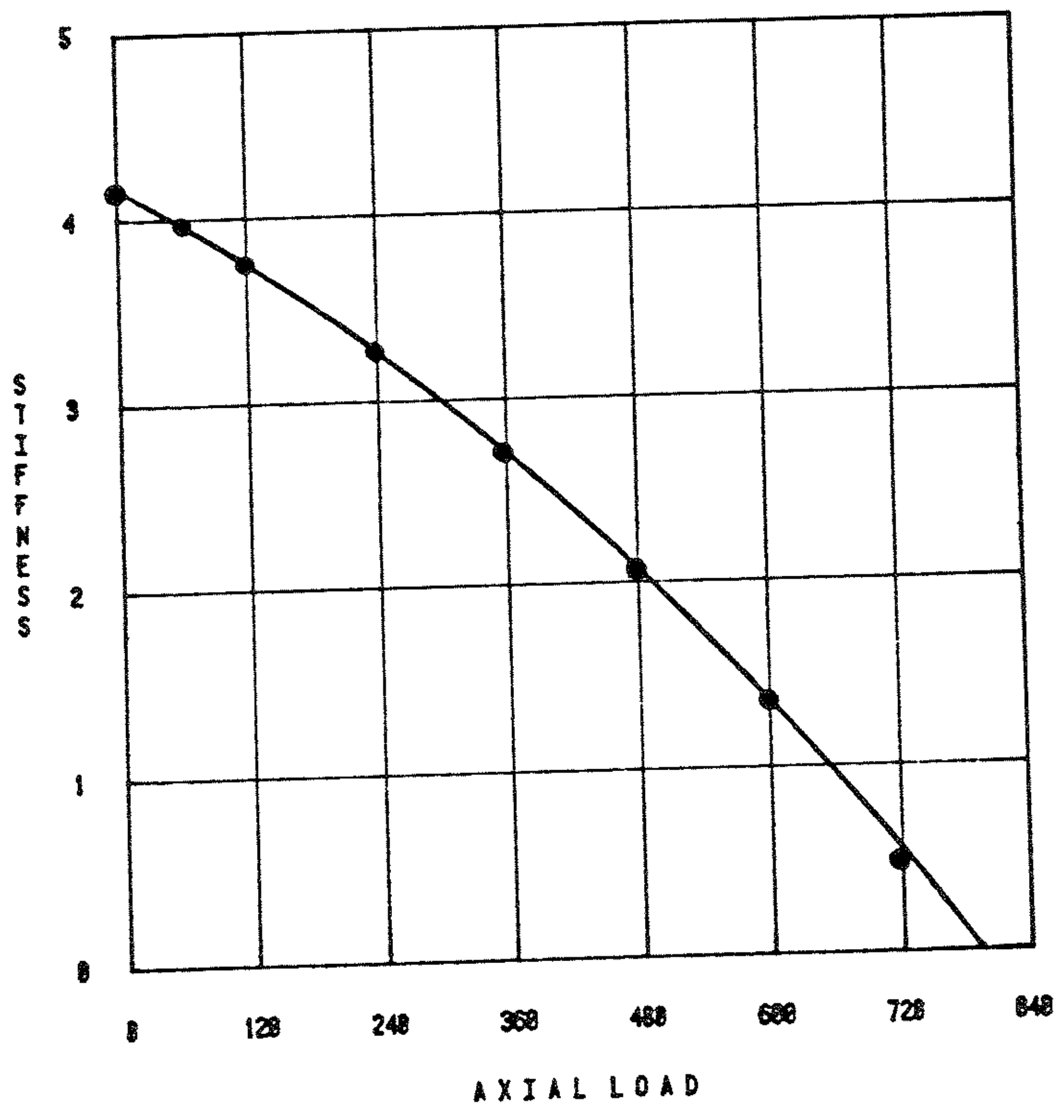

Fig. 8. Comparison of results of two-dimensional finite elasticity model with Haringx's theory. (without roll-off).

Beam propreties

$E = 10000.$

$G = 50$

Material properties

$\lambda^{*} = 2666.67$

$\mu^{*} = 4000.$

$\nu^{*} = .25$

$G^{*} = 50. + \frac{P}{A}$

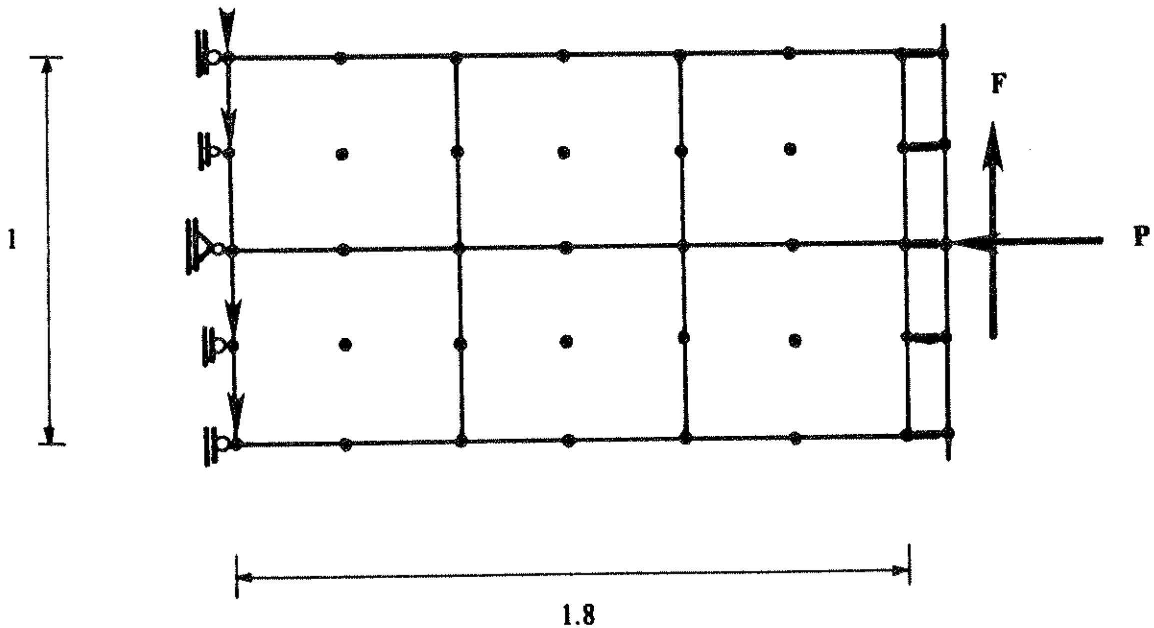

Fig. 9. Material properties and mesh for example 2.

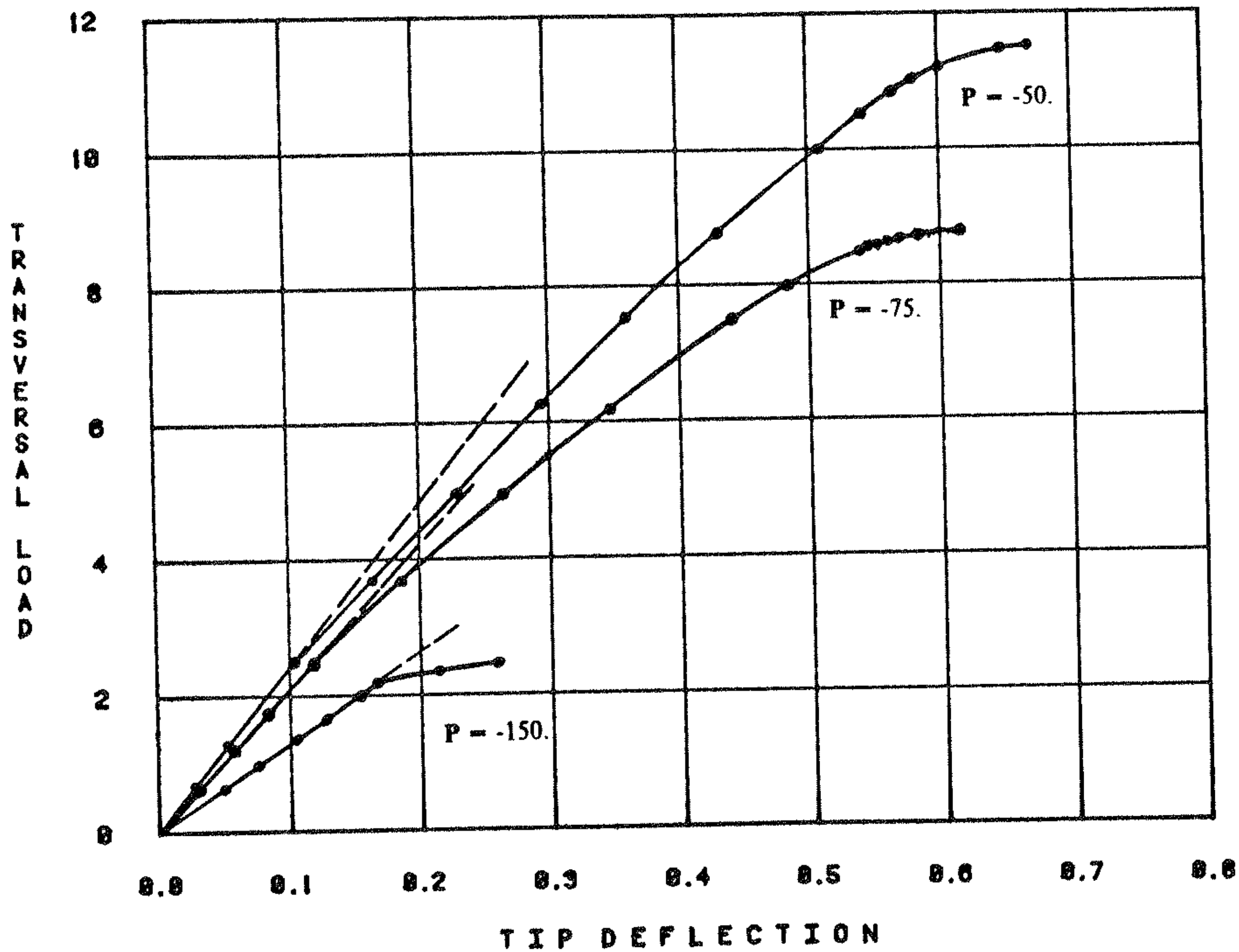

Fig. 10. Instability produced by roll-off: Two-dimensional finite elasticity model.

APPENDIX I

Material instability. Experimental results

The possibility of an instability phenomenon for certain class of non linear materials when subjected to a state of simple shear, has been pointed out by Truesdell ([18] and references therein). This type of instability, material instability in Truesdell's terminology, is due to the form of the constitutive equations of the material rather than to the geometry of the problem.

The phenomenon can be illustrated by considering the following generalization of the strain energy corresponding to the Mooney-Rivlin model

$$W = \frac{1}{2}\mu\left[(\frac{1}{2}+\beta)(I_1-3) + (\frac{1}{2}-\beta)(I_2-3) - \frac{1}{2\gamma}(I_2-3)^2 \right] \qquad (I.1)$$

where $\mu > 0$, $-\frac{1}{2} \leq \beta \leq \frac{1}{2}$ and $\gamma > 0$ to ensure the positive definiteness of W.

For this type of material, the generalized shear modulus in a state of simple shear takes the form [18]

$$\hat{\mu} = \frac{\sigma_{12}}{\kappa} = \mu \left[1 - \frac{\kappa^2}{\gamma} \right] \qquad (I.2)$$

where $\kappa = \tan\alpha$, α being the shearing angle, and σ_{12} the shear stress.

A collapse in shear will occur whenever $\frac{d\sigma_{12}}{d\kappa} = 0$. From (I.2) we find the critical value

$$\kappa_{crit} = \left[\frac{\gamma}{3} \right]^{\frac{1}{2}} \qquad (I.3)$$

The example shows that the actual occurence of this type of instability is a possibility that must be taken into account. The simple experimental test described below, was conducted to assess wehether the discussed instability phenomenon should be expected in the behavior of a typical multilayer elastomeric bearing.

Experimental test.

The experimental test was designed to subject a single layer of an elastomeric bearing to a combined state of compression and shear deformation. The type of bearing chosen had been tested previously at the Earthquaque Engineering Researh Center of the University of California, Berkeley, showing an instability phenomenon of the type described in the introduction of this report. Thus, if the phenomenon were to be attributable to a form of material instability, it would be expected to appear in the course of the test.

The experimental set-up is shown in Fig.I.1 to Fig.I.4. The shear load is controlled by a universal testing machine, allowing for a high degree of accuracy. The axial load by a hydraulic jack with an estimate error of 5% to 8%. The disposition of the L.V.D.T. used to control the axial and shear deformation is also illustrated in the attached figures.

The specimen was subjected to a several axial loads, and shear deformations up to 250%, a rather high amount of shear.

It should be noted that it is extremely difficult to reproduce experimentally the conditions of a homogeneous state of shear deformation. The reason for this is the lack of control in the normal stresses which are necessary to reproduce the Poynting effect [11]. Thus, the experimental state of deformation is only an approximation of the theoratical state of combined axial and shear deformation.

The experimental results obtained from the test are plotted in Figs.I.5 to I.8. From them, the following conclusions can be drawn:

(1) It appears to be no indication of a material instability phenomenon. In fact, as the shear strain is increased, a completely opposite effect of stiffening can be observed for large amounts of shear.

(2) Within a large range of shear deformation, the relationship beteween shear load and shear displacement is approximately linear.

(3) The apparent shear modulus for a single layer is highly insensitive to the value of applied axial load.

This conclusions show that the hypothesis of material instability, although theoretically appealing, should be ruled out in the present case. Furthermore, they confirm the usual assumption of a linear relationship beteween shear load and shear deformation. In the context of a more elaborate theory, they also seem to suggest the constituive assumption of the Mooney-Rivlin model for the rubber.

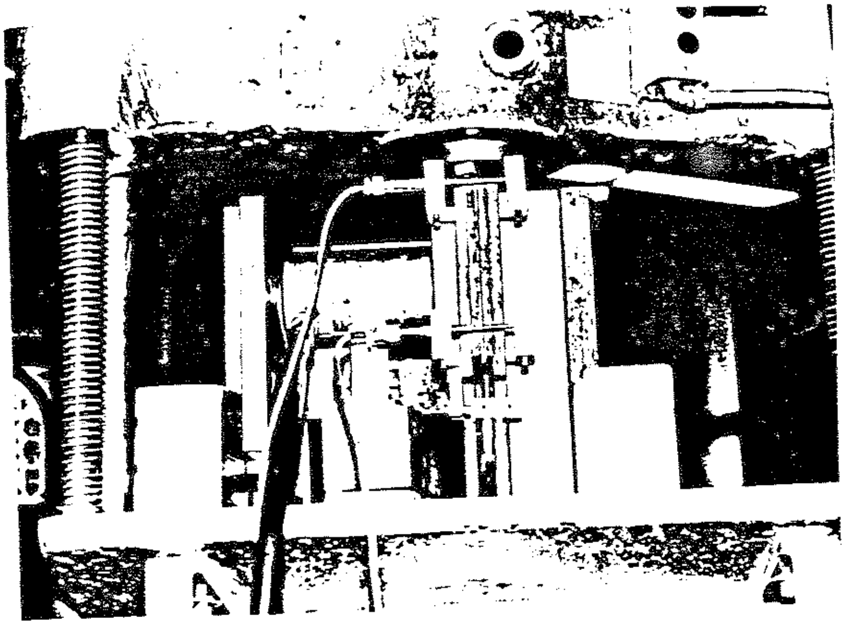

Fig. I.1.

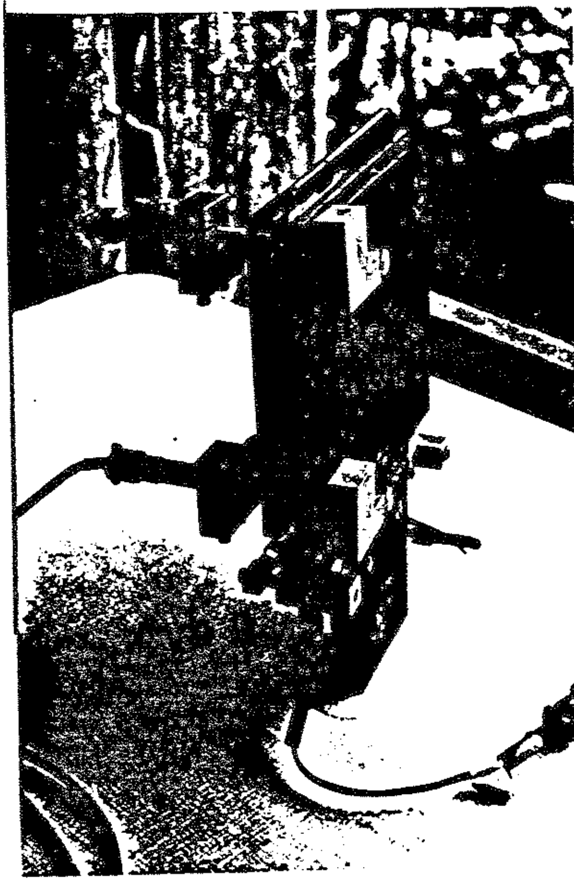

Fig. I.2.

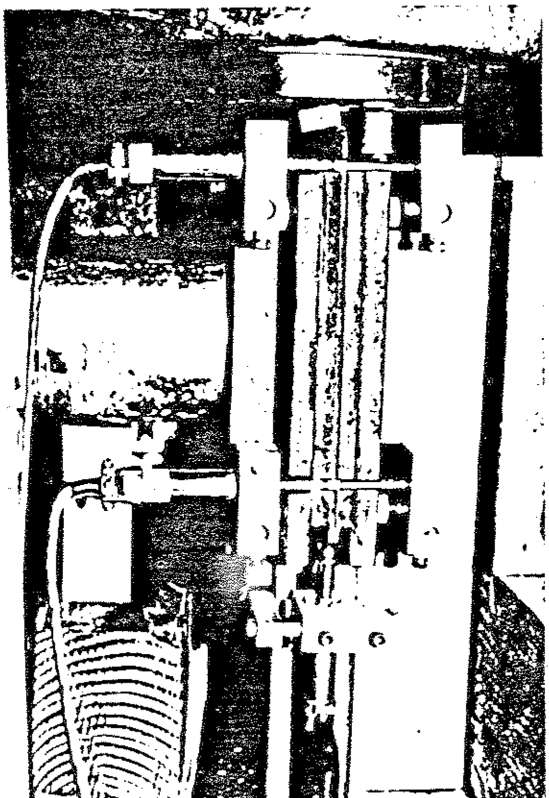

Fig. I.3.

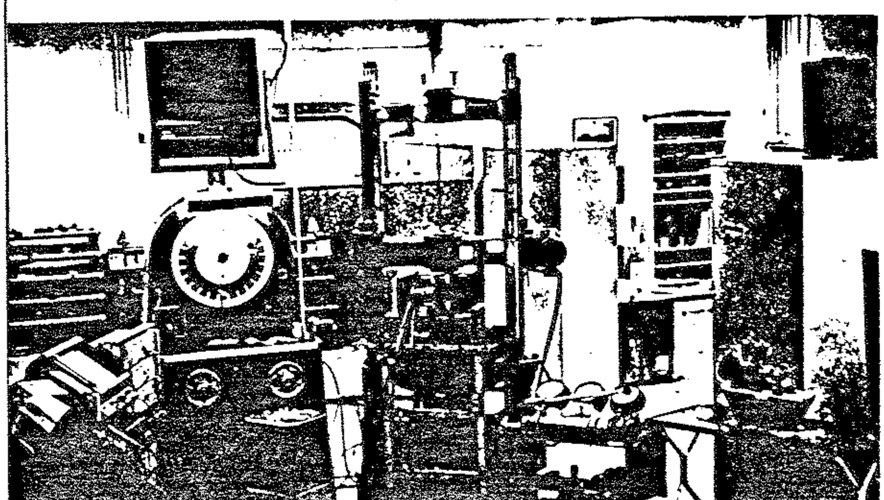

Fig. I.4.

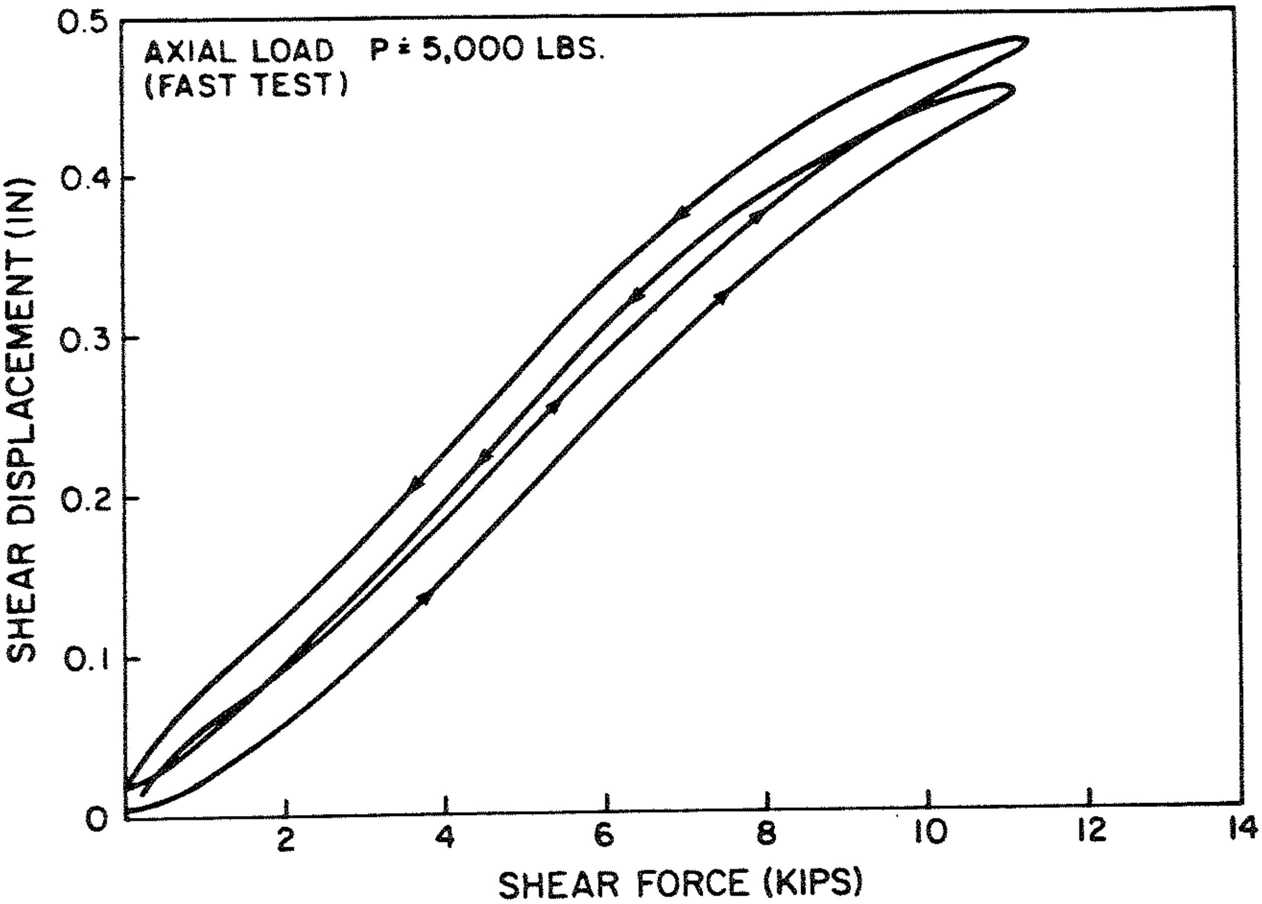

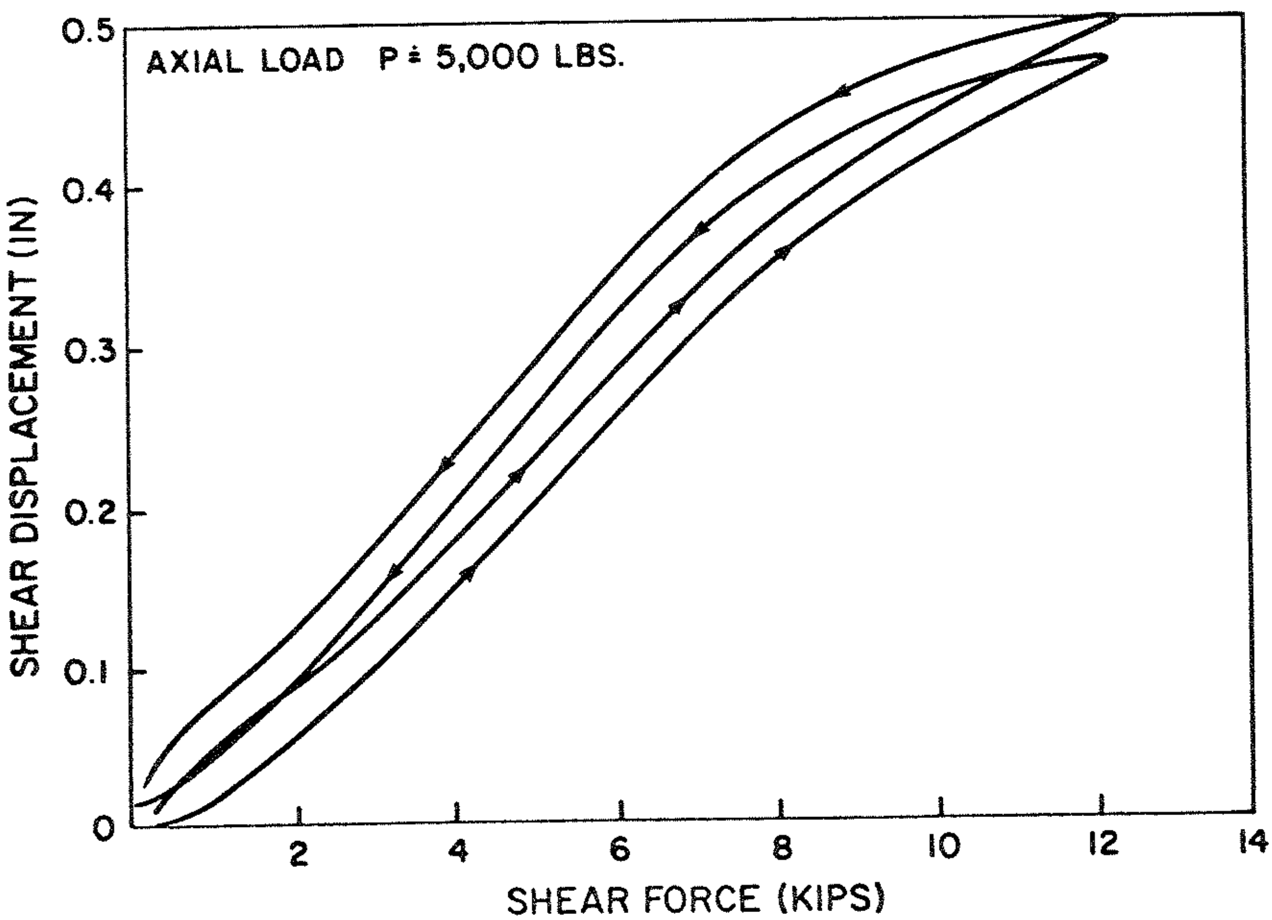

Figs. I.5. and I.6. Experimental results.

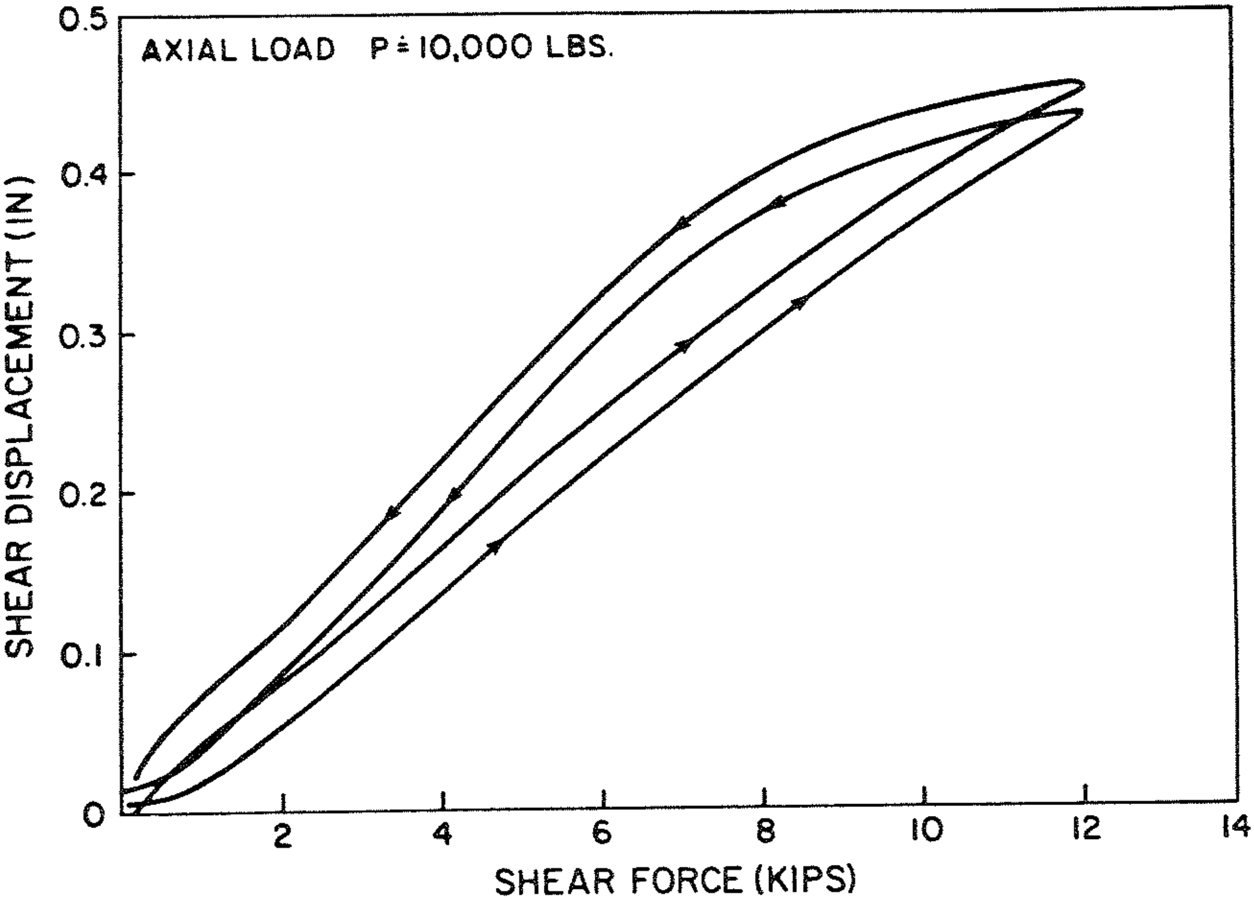

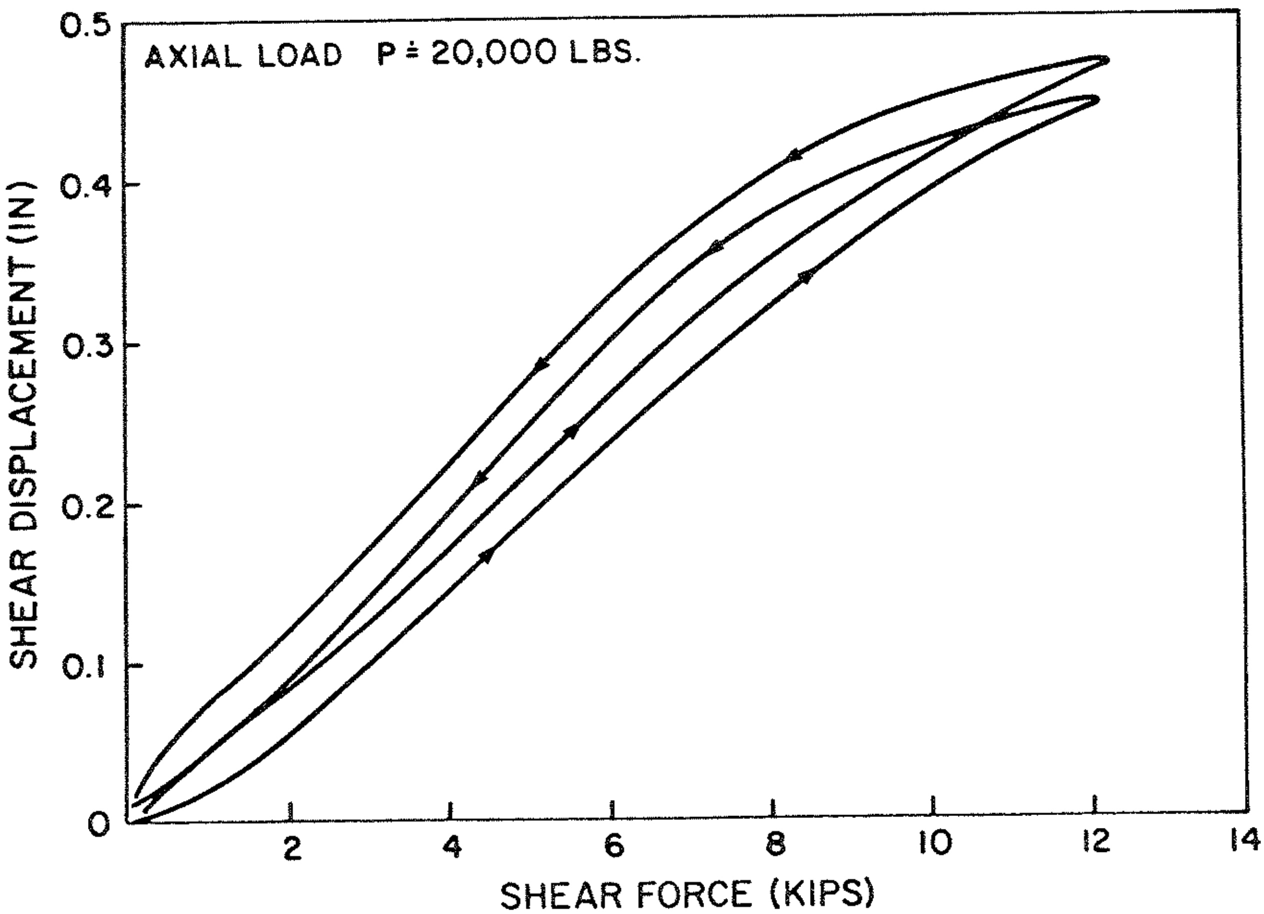

Figs. I.7. and I.8. Experimental results.

APPENDIX II

Finite Elasticity approach to Haringx's theory.

It will be shown in this appendix, that the equilibrium equations in Haringx's treatment follow from the equations of equilibrium of two-dimensional finite elasticity whenever the assumptions of beam theory hold. Furthermore, the derivation yields the consistent definition of the resultant forces acting on an arbitrary deformed cross section, in terms of the different stress tensors.

Kinematics.

Consider a beam with cross sectional area A and length L. As in section 4.1, the reference configuration $[0,L]XA$ is denoted by B, and by $\mathbf{x} = \Phi(\mathbf{X})$ the the final position of a particle located at **X** in the undeformed configuration B of the beam.

Neglecting the warping of the section, the basic kinematic assumption is that a section normal to the center line in the undeformed configuration remains normal to the deformed center line. With the notation of Fig.II.1, the coordinate expression for the deformation map is

$$\begin{aligned} x_1 &= X_1 + u(X_1) - X_2 \sin\psi(X_1) \\ x_2 &= v(X_1) + X_2 \cos\psi(X_1) \end{aligned} \qquad \text{(II.1)}$$

and the components $F_{iI} = \dfrac{\partial x_i}{\partial X_I}$ of the deformation gradient **F** are given by

$$\mathbf{F} = \begin{bmatrix} 1+u'-X_2\psi'\cos\psi & -\sin\psi \\ v'-X_2\psi'\sin\psi & \cos\psi \end{bmatrix} \qquad \text{(II.2)}$$

An element of area dA in an undeformed cross section, with unit normal $\hat{\mathbf{N}} = (1,0)$, is mapped onto the element of area da with unit normal $\hat{\mathbf{n}}$. If $J=\det(\mathbf{F})$ the basic relation

$$da\,\hat{\mathbf{n}} = J dA\, \mathbf{F}^{-t}\hat{\mathbf{N}} \qquad \text{(II.3)}$$

shows that the areas are preserved; i.e: $da = dA$ and that $\hat{\mathbf{n}} = (\cos\psi, \sin\psi)$. Similarly, the unit vector $\hat{\mathbf{L}} = (0,1)$ perpendicular to $\hat{\mathbf{N}}$, is mapped onto the vector $\hat{\mathbf{l}} = \mathbf{F}\hat{\mathbf{L}} = (-\sin\psi, \cos\psi)$.

The Lagrangian strain tensor [11] is defined in terms of the deformation gradient $\mathbf{F}$ by

$$\mathbf{E} = \frac{1}{2}[\mathbf{F}^t\mathbf{F} - \mathbf{1}] \tag{II.4}$$

The substitution of (II.2) into (A.4) shows that the component $E_{22} = 0$. The same conclusion holds in the linear theory when the linearization of equations (II.1) is assumed. The exact solution of the bending problem in the case of small displacements indicates that this conclusion is not exactly true, but rather a consequence of the approximate character of (II.1).

Resultant forces on an arbitrary cross section

Let us denote by $\mathbf{P}$ and σ the first Piola- Kirchhoff and Cauchy stress tensors, respectively [11]. The force vector acting on the element of area da, with unit normal $\hat{\mathbf{n}}$, of a deformed cross section is given by

$$d\mathbf{F} = \sigma\hat{\mathbf{n}}da = \mathbf{P}\hat{\mathbf{N}}dA \tag{II.5}$$

where dA and $\hat{\mathbf{N}}$ are the corresponding element of area and unit normal in the undeformed cross section. The normal force and the tangential force acting on da are then

$$\begin{aligned} dF_n &= \hat{\mathbf{n}}.(\sigma\hat{\mathbf{n}})da = \hat{\mathbf{n}}.(\mathbf{P}\hat{\mathbf{N}})dA \\ dF_t &= \hat{\mathbf{l}}.(\sigma\hat{\mathbf{n}})da = \hat{\mathbf{l}}.(\mathbf{P}\hat{\mathbf{N}})dA \end{aligned} \tag{II.6}$$

where $\hat{\mathbf{l}}$ and $\hat{\mathbf{L}}$ are normal to $\hat{\mathbf{n}}$ and $\hat{\mathbf{N}}$, respectively. Therefore, the resultant forces acting on a deformed cross section of the beam are

$$N = \int_A (\mathbf{P}\hat{\mathbf{N}}).\hat{\mathbf{n}}dA \quad V = \int_A (\mathbf{P}\hat{\mathbf{N}}).\hat{\mathbf{l}}dA \quad M = -\int_A X_2(\mathbf{P}\hat{\mathbf{N}}).\hat{\mathbf{n}}dA \tag{II.7}$$

From the expressions for $\hat{\mathbf{N}}$, $\hat{\mathbf{n}}$, and $\hat{\mathbf{l}}$ it follows that

$$\begin{aligned} N &= \cos\psi\int_A P_{11}dA + \sin\psi\int_A P_{21}dA \\ V &= -\sin\psi\int_A P_{11}dA + \cos\psi\int_A P_{21}dA \end{aligned} \tag{II.8}$$

or equivalently

$$\int_A P_{11}dA = \cos\psi N - \sin\psi V, \quad \int_A P_{21}dA = \sin\psi N + \cos\psi V \tag{II.9}$$

No approximation is involved in equations (II.6) through (II.9), they are consistent with the kinematic assumption expressed by equation (II.1)

The relationship to first order approximation, between the different stress components is considered next.

Linearization. Relations connecting stress tensors.

We will assume that the axial displacement u of the center line and its derivative u' are small enough † so that the contribution of the terms containing u' can be neglected. This assumption is particularly reasonable in the case of multilayer elastomeric bearings.

Let **S** be the second Piola-Kirchhoff stress tensor defined by

$$\mathbf{S} = \mathbf{F}^{-1}\mathbf{P} = J\mathbf{F}^{-1}\sigma\mathbf{F}^{-t} \tag{II.10}$$

from equation (II.2) we find the first order relationship

$$\mathbf{P} = \sigma\begin{bmatrix} 1 & -v' \\ \psi & 1 \end{bmatrix} = \begin{bmatrix} 1 & -\psi \\ v' & 1 \end{bmatrix}\mathbf{S} \tag{II.11}$$

and from (II.8) we obtain the expressions

$$\int_A P_{11}dA = N - \psi V \qquad \int_A P_{21}dA = \psi N + V \tag{II.12}$$

$$\int_A S_{11}dA = N \qquad \int_A S_{12} = -(v'-\psi)N + V \tag{II.13}$$

We note that (II.12) and (II.13) provide a physical interpretation for the components of **P** and **S**. In particular, if σ and τ are the normal and tangential stresses acting on an element of area da of the deformed cross section of the beam, equation (II.13) states that

$$S_{11} = \sigma \qquad S_{12} = \tau - (v'-\psi)\sigma \tag{II.14}$$

in addition, since $\hat{\mathbf{n}}.(\mathbf{P}\hat{\mathbf{n}}) = \sigma$, the expression in (II.7) for the bending moment reduces to

$$M = -\int_A S_{11}X_2dA \tag{II.15}$$

In order to obtain an first order estimate of P_{12} recall from linear elasticity, that the exact solution for bending of a beam with no distributed loads shows that $\sigma_{22} = 0$. Thus, it is reasonable to assume that the stresses normal to the deformed center line can be neglected. This

† more precisely: $||u|| = \max\limits_{0\leqslant x\leqslant L} |u| + \max\limits_{0\leqslant x\leqslant L} |u'|$ is small.

assumption together with equation (II.11) yields the first order estimates

$$\sigma_{22} = 2\psi\sigma_{12}\,,\quad P_{22} = (v'-2\psi)\sigma_{12}\,,\quad S_{22} = 2(\psi - v')\sigma_{12} \tag{II.16}$$

Therefore, the term ψS_{22} can be neglected in a first order approximation. Equations (II.11) and (II.12) show that

$$\int_A P_{12} dA = \int_A S_{12} dA = V - (v'-\psi)N \tag{II.17}$$

If the deformation due to shear can be neglected, $\psi = v'$ and equation (II.17) yields the expression

$$V = \int_A S_{12} dA$$

However, when the shear deformation is important, as in the case of elastomeric bearings, this simple relation no longer holds and (II.17) must be used.

The equations of equilibrium

The material form of the equations of equilibrium in finite elasticity [12] is

$$Div(\mathbf{P}) + \rho_o \bar{\mathbf{b}} = 0 \tag{II.18}$$

where ρ_o and $\bar{\mathbf{b}}$ are the density and body forces referred to the undeformed (reference) configuration. Assuming that no distributed loads exists and zero body forces, the integration of equations (II.18) through the undeformed cross sectional area together with (II.12) and (II.15) give the system of equations

$$\begin{aligned} &[\,N - \psi V\,]' = 0 \\ &[\,\psi N + V\,]' = 0 \\ &[\,M' + V - (v'-\psi)N\,] = 0 \end{aligned} \tag{II.19}$$

The same result is obtained if instead of equation (II.18) its variational formulation, the principle of virtual work, is used. The expression in terms of the first Piola-Kirchhoff stress tensor and its dual measure of deformation, the deformation gradient, is particularly convenient if this approach is followed.

Either by integration of equations (II.19) or by the principle of virtual work, we find the expressions

$$N - \psi V = -P \qquad V + \psi N = -Q$$

where P is the axial load and V the transversal load applied at the end of the beam. Thus an equivalent statement of the equilibrium equations (II.16) is

$$\begin{aligned} N &= -P - \psi Q \\ V &= \psi P - Q \\ M'' &+ Pv'' = 0 \end{aligned} \tag{II.20}$$

Finally, the two dimensional constitutive model proposed in section 3. of this report, leads to the classical equations

$$M = EI\psi' \qquad V = GA_s(v'-\psi)$$

and their substitution into (II.20) yields the equation of buckling due to Haringx

$$\frac{EI}{1+\frac{P}{GA_s}} \frac{d^4v}{dx^4} + P \frac{d^2v}{dx^4} = 0 \qquad 0<x<L \tag{II.21}$$

where for simplicity in the notation we have set $x = X_1$.

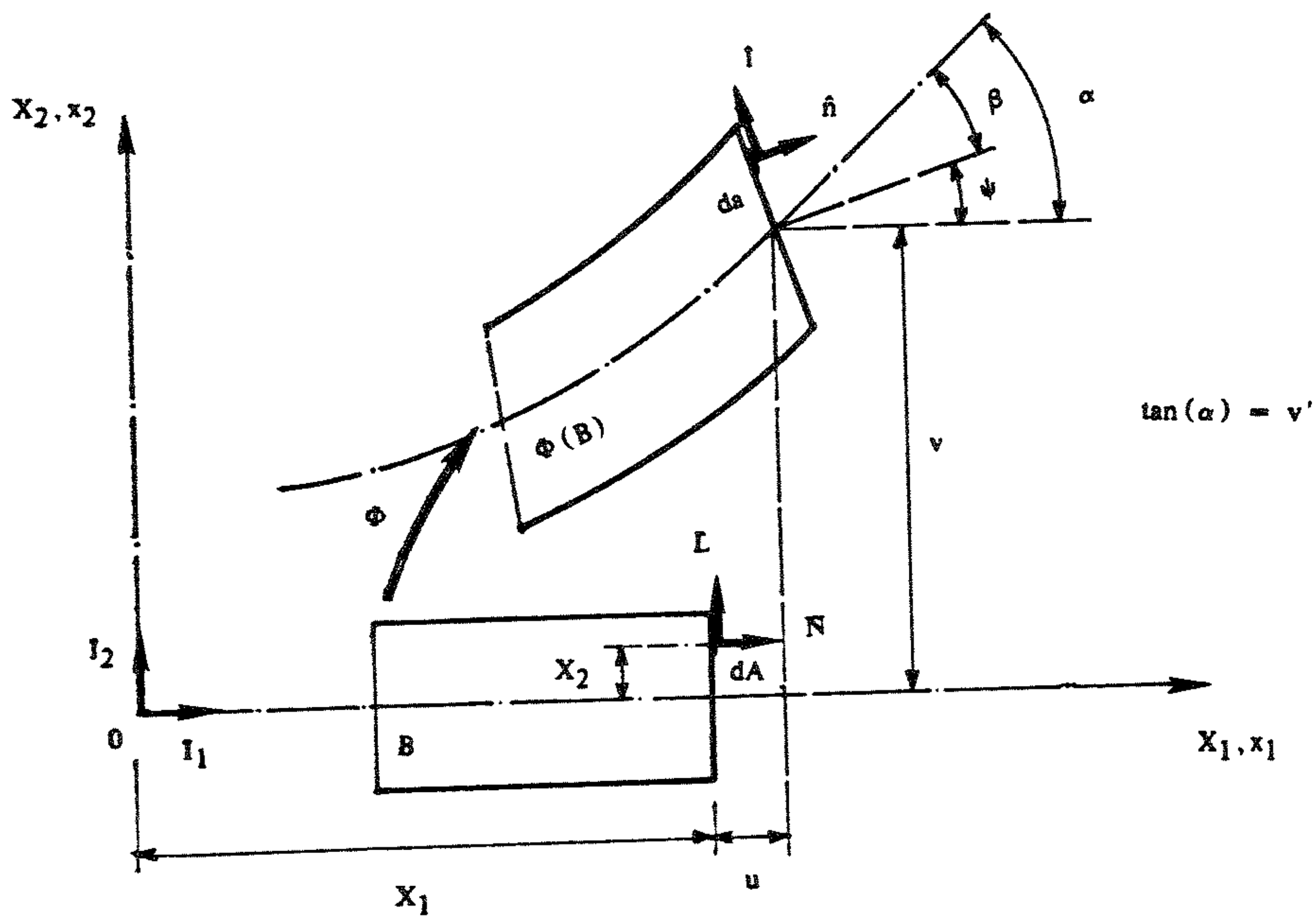

Fig.I.1. Kinematics of the deformation of a beam.